EURANDOM PREPRINT SERIES

2018-011

July 13, 2018

Breaking of ensemble equivalence for perturbed Erdős Rényi random graphs

F. den Hollander, M. Mandjes, A. Roccaverde, N. Starreveld
ISSN 1389-2355

Breaking of ensemble equivalence for perturbed Erdős-Rényi random graphs

F. den Hollander [1]
M. Mandjes [2]
A. Roccaverde [3]
N.J. Starreveld [4]

July 13, 2018

Abstract

In a previous paper we analysed a simple undirected random graph subject to constraints on the total number of edges and the total number of triangles. We considered the dense regime in which the number of edges per vertex is proportional to the number of vertices. We showed that, as soon as the constraints are *frustrated*, i.e., do not lie on the Erdős-Rényi line, there is breaking of ensemble equivalence, in the sense that the specific relative entropy per edge of the *microcanonical ensemble* with respect to the *canonical ensemble* is strictly positive in the limit as the number of vertices tends to infinity. In the present paper we analyse what happens near the Erdős-Rényi line. It turns out that the way in which the specific relative entropy tends to zero depends on whether the total number of triangles is slightly larger or slightly smaller than typical. We identify what the constrained random graph looks like asymptotically in the microcanonical ensemble.

MSC 2010: 05C80, 60K35, 82B20.
Key words: Erdős-Rényi random graph, Gibbs ensembles, relative entropy, graphon, breaking of ensemble equivalence, constrained random graph.

Acknowledgements: The research in this paper was supported through NWO Gravitation Grant NETWORKS 024.002.003. The authors are grateful to V. Patel and H. Touchette for helpful discussions. FdH, AR and NJS are grateful for hospitality at the International Centre for Theoretical Sciences in Bangalore, India, as participants of the program on *Large Deviation Theory in Statistical Physics: Recent Advances and Future Challenges* in the Fall of 2017.

1 Introduction

In this paper we analyse random graphs that are subject to *constraints*. Statistical physics prescribes what probability distribution on the set of graphs we should choose when we want to model a given type of constraint [12]. Two important choices are:

(1) The *microcanonical ensemble*, where the constraints are *hard* (i.e., are satisfied by each individual graph).

[1]Mathematical Institute, Leiden University, P.O. Box 9512, 2300 RA Leiden, The Netherlands
denholla@math.leidenuniv.nl
[2]Korteweg de-Vries Institute, University of Amsterdam, P.O. Box 94248, 1090 GE Amsterdam, The Netherlands
m.r.h.mandjes@uva.nl
[3]Mathematical Institute, Leiden University, P.O. Box 9512, 2300 RA Leiden, The Netherlands
a.roccaverde@math.leidenuniv.nl
[4]Korteweg de-Vries Institute, University of Amsterdam, P.O. Box 94248, 1090 GE Amsterdam, The Netherlands
n.j.starreveld@uva.nl

(2) The *canonical ensemble*, where the constraints are *soft* (i.e., hold as ensemble averages, while individual graphs may violate the constraints).

For random graphs that are large but finite, the two ensembles are obviously different and, in fact, represent different empirical situations. Each ensemble represents the unique probability distribution with *maximal entropy* respecting the constraints. In the limit as the size of the graph diverges, the two ensembles are traditionally *assumed* to become equivalent as a result of the expected vanishing of the fluctuations of the soft constraints, i.e., the soft constraints are expected to behave asymptotically like hard constraints. This assumption of *ensemble equivalence* is one of the corner stones of statistical physics, but it does *not* hold in general (see [32] for more background).

In a series of papers the question of possible breaking of ensemble equivalence was investigated for various choices of the constraints, including the degree sequence and the total number of edges, wedges and triangles. Both the *sparse regime* (where the number of edges per vertex remains bounded) and the *dense regime* (where the number of edges per vertex is of the order of the number of vertices) have been considered. The effect of *community structure* on ensemble equivalence has been investigated as well. Relevant references are [13], [14], [15], [30] and [31]. In [15] we considered a random graph subject to constraints on the total number of edges and the total number of triangles, in the dense regime. With the help of *large deviation theory for graphons* (see [9]), we derived a variational formula for $s_\infty = \lim_{n\to\infty} n^{-2} s_n$, where n is the number of vertices and s_n is the *relative entropy* of the microcanonical ensemble with respect to the canonical ensemble. We found that $s_\infty > 0$ when the constraints are *frustrated*. In the present paper we analyse the behaviour of s_∞ when the constraints are close to but different from those of the Erdős-Rényi random graph, and we identify what the constrained random graph looks like asymptotically in the microcanonical ensemble. It turns out that the behaviour changes when the total number of triangles is larger, respectively, smaller than that of the Erdős-Rényi random graph with a given total number of edges.

While breaking of ensemble equivalence is a relatively new concept in the theory of random graphs, there are many studies on the asymptotic structure of random graphs. In the pioneering work [9], followed by [20], the large deviation principle for dense Erdős-Rényi random graphs was proven and the asymptotic structure of constrained Erdős-Rényi random graphs was described as the solution of a variational problem. In the past few years significant progress has been made regarding sparse random graphs as well. We refer the reader to [8], [10], [21] and [36]. Two other random graph models that have been extensively studied are the following:

- *Exponential random graphs*, which are related to the canonical ensemble, were introduced in the physics literature (see [23] and references therein), and were subsequently analysed in detail in [3] and [7]. In [3] the mixing time of the Ising model subject to Glauber dynamics was investigated, and it was shown that exponential random graphs behave asymptotically like Erdős-Rényi random graphs with a biased parameter. In [7] this result was generalised with the help of the machinery developed in [9], resulting in an asymptotic expression for the logarithm of the partition function in terms of a variational problem. iIt was further shown that in the edge-triangle model a phase transition occurs for specific values of the parameters, which is defined as a discontinuity in the derivative of the logarithm of the partition function. The existence of phase transitions for exponential random graphs was investigated further in [28] and [33], and for directed graphs in [2]. An analysis of sparse exponential random graphs was carried out in [35].

- *Constrained exponential random graphs* have received a lot of attention in the literature. We refer the reader to [1], [17], [19] and [34] for a detailed description and analysis. A stream of research that is relevant for the present paper concerns the asymptotic description of the structure of graphs drawn from the microcanonical ensemble with a constraint on the edge density and the triangle density. In [27] the behaviour of random graphs with edge and triangle densities close to the Erdős-Rényi line was studied. The scaling behaviour was studied via a bound on the entropy function. In one of the results in the present paper, we rigorously prove the results of [27] and determine the exact structure of constrained random graphs close to the Erdős-Rényi line. The same question was investigated in [22] for a constraint on the edge density and the

triangle density close to the lower boundary of the admissibility region. In [18], through extensive simulations, curves in the admissibility region were determined where phase transitions occur in the structure of the constrained random graphs.

The remainder of this paper is organised as follows. In Section 2 we define the two ensembles, give the definition of equivalence of ensembles in the dense regime, and recall some basic facts about graphons. In Section 2.4 we recall the *variational representation* of s_∞ derived in [15] when the constraints are on the total numbers of subgraphs drawn from a finite collection of subgraphs. We also recall the analysis of s_∞ in [15] for the special case where the subgraphs are the edges and the triangles. In Section 3 we state our main theorems. Proofs are given in Sections 4 and 5.

2 Definitions and preliminaries

In Section 2.1 we give the formal definition of the two ensembles we are interested in and give our definition of equivalence of ensembles in the dense regime. In Section 2.2 we recall some basic facts about *graphons*, in Section 2.3 we present some basic properties of the canonical ensemble and in Section 2.4 we give a variational characterisation of ensemble equivalence proven in [15].

2.1 Microcanonical ensemble, canonical ensemble, relative entropy

For $n \in \mathbb{N}$, let $\mathcal{G}_n$ denote the set of all $2^{\binom{n}{2}}$ simple undirected graphs with n vertices. Any graph $G \in \mathcal{G}_n$ can be represented by a symmetric $n \times n$ matrix with elements

$$h^G(i,j) := \begin{cases} 1 & \text{if there is an edge between vertex } i \text{ and vertex } j, \\ 0 & \text{otherwise.} \end{cases} \tag{2.1}$$

Let $\vec{C}$ denote a vector-valued function on $\mathcal{G}_n$. We choose a specific vector $\vec{C}^*$, which we assume to be *graphical*, i.e., realisable by at least one graph in $\mathcal{G}_n$. For this $\vec{C}^*$ the *microcanonical ensemble* is the probability distribution $\mathrm{P}_{\mathrm{mic}}$ on $\mathcal{G}_n$ with *hard constraint* $\vec{C}^*$ defined as

$$\mathrm{P}_{\mathrm{mic}}(G) := \begin{cases} 1/\Omega_{\vec{C}^*}, & \text{if } \vec{C}(G) = \vec{C}^*, \\ 0, & \text{otherwise,} \end{cases} \qquad G \in \mathcal{G}_n, \tag{2.2}$$

where

$$\Omega_{\vec{C}^*} := |\{G \in \mathcal{G}_n \colon \vec{C}(G) = \vec{C}^*\}| \tag{2.3}$$

is the number of graphs that realise $\vec{C}^*$. The *canonical ensemble* $\mathrm{P}_{\mathrm{can}}$ is the unique probability distribution on $\mathcal{G}_n$ that maximises the *entropy*

$$S_n(\mathrm{P}) := -\sum_{G \in \mathcal{G}_n} \mathrm{P}(G) \log \mathrm{P}(G) \tag{2.4}$$

subject to the *soft constraint* $\langle \vec{C} \rangle = \vec{C}^*$, where

$$\langle \vec{C} \rangle := \sum_{G \in \mathcal{G}_n} \vec{C}(G)\, \mathrm{P}(G). \tag{2.5}$$

This gives the formula [16]

$$\mathrm{P}_{\mathrm{can}}(G) := \frac{1}{Z(\vec{\theta}^*)}\, \mathrm{e}^{H(\vec{\theta}^*, \vec{C}(G))}, \qquad G \in \mathcal{G}_n, \tag{2.6}$$

with

$$H(\vec{\theta}^*, \vec{C}(G)) := \vec{\theta}^* \cdot \vec{C}(G), \qquad Z(\vec{\theta}^*) := \sum_{G \in \mathcal{G}_n} \mathrm{e}^{\vec{\theta}^* \cdot \vec{C}(G)}, \tag{2.7}$$

denoting the *Hamiltonian* and the *partition function*, respectively. In (2.6)–(2.7) the parameter $\vec{\theta}^*$, which is a real-valued vector whose size is equal to the number of constraints, must be set to the unique value that realises $\langle \vec{C} \rangle = \vec{C}^*$. As a Lagrange multiplier, $\vec{\theta}^*$ always exists, but uniqueness is non-trivial. In the sequel we will only consider examples where the gradients of the constraints in (2.5) are linearly independent vectors. Consequently, the Hessian matrix of the entropy of the canonical ensemble in (2.6) is a positive-definite matrix, which implies uniqueness.

The *relative entropy* of $\mathrm{P}_{\mathrm{mic}}$ with respect to $\mathrm{P}_{\mathrm{can}}$ is defined as

$$S_n(\mathrm{P}_{\mathrm{mic}} \mid \mathrm{P}_{\mathrm{can}}) := \sum_{G \in \mathcal{G}_n} \mathrm{P}_{\mathrm{mic}}(G) \log \frac{\mathrm{P}_{\mathrm{mic}}(G)}{\mathrm{P}_{\mathrm{can}}(G)}. \tag{2.8}$$

For any $G_1, G_2 \in \mathcal{G}_n$, $\mathrm{P}_{\mathrm{can}}(G_1) = \mathrm{P}_{\mathrm{can}}(G_2)$ whenever $\vec{C}(G_1) = \vec{C}(G_2)$, i.e., the canonical probability is the same for all graphs with the same value of the constraint. We may therefore rewrite (2.8) as

$$S_n(\mathrm{P}_{\mathrm{mic}} \mid \mathrm{P}_{\mathrm{can}}) = \log \frac{\mathrm{P}_{\mathrm{mic}}(G^*)}{\mathrm{P}_{\mathrm{can}}(G^*)}, \tag{2.9}$$

where G^* is *any* graph in $\mathcal{G}_n$ such that $\vec{C}(G^*) = \vec{C}^*$ (recall that we assumed that $\vec{C}^*$ is realisable by at least one graph in $\mathcal{G}_n$). All the quantities above depend on n. In order not to burden the notation, we exhibit this n-dependence only in the symbols $\mathcal{G}_n$ and $S_n(\mathrm{P}_{\mathrm{mic}} \mid \mathrm{P}_{\mathrm{can}})$. When we pass to the limit $n \to \infty$, we need to specify how $\vec{C}(G)$, $\vec{C}^*$ and $\vec{\theta}^*$ are chosen to depend on n. We refer the reader to [15] where this issue has been discussed in detail.

Definition 2.1 *In the dense regime, if*

$$s_\infty := \lim \frac{1}{n^2} S_n(\mathrm{P}_{\mathrm{mic}} \mid \mathrm{P}_{\mathrm{can}}) = 0, \tag{2.10}$$

then $\mathrm{P}_{\mathrm{mic}}$ *and* $\mathrm{P}_{\mathrm{can}}$ *are said to be equivalent.*

Remark 2.2 In [31], which was concerned with the *sparse regime*, the relative entropy was divided by n (the number of vertices). In the *dense regime*, however, it is appropriate to divide by n^2 (the order of the number of edges).

2.2 Graphons

There is a natural way to embed a simple graph on n vertices in a space of functions called *graphons*. Let W be the space of functions $h\colon [0,1]^2 \to [0,1]$ such that $h(x,y) = h(y,x)$ for all $(x,y) \in [0,1]^2$. A finite simple graph G on n vertices can be represented as a graphon $h^G \in W$ in a natural way as (see Figure 1)

$$h^G(x,y) := \begin{cases} 1 & \text{if there is an edge between vertex } \lceil nx \rceil \text{ and vertex } \lceil ny \rceil, \\ 0 & \text{otherwise.} \end{cases} \tag{2.11}$$

The space of graphons W is endowed with the *cut distance*

$$d_\square(h_1, h_2) := \sup_{S,T \subset [0,1]} \left| \int_{S \times T} \mathrm{d}x \, \mathrm{d}y \, [h_1(x,y) - h_2(x,y)] \right|, \qquad h_1, h_2 \in W. \tag{2.12}$$

On W there is a natural equivalence relation $\equiv$. Let Σ be the space of measure-preserving bijections $\sigma\colon [0,1] \to [0,1]$. Then $h_1(x,y) \equiv h_2(x,y)$ if $h_1(x,y) = h_2(\sigma x, \sigma y)$ for some $\sigma \in \Sigma$. This equivalence relation yields the quotient space $(\tilde{W}, \delta_\square)$, where $\delta_\square$ is the metric defined by

$$\delta_\square(\tilde{h}_1, \tilde{h}_2) := \inf_{\sigma_1, \sigma_2 \in \Sigma} d_\square(h_1^{\sigma_1}, h_2^{\sigma_2}), \qquad \tilde{h}_1, \tilde{h}_2 \in \tilde{W}. \tag{2.13}$$

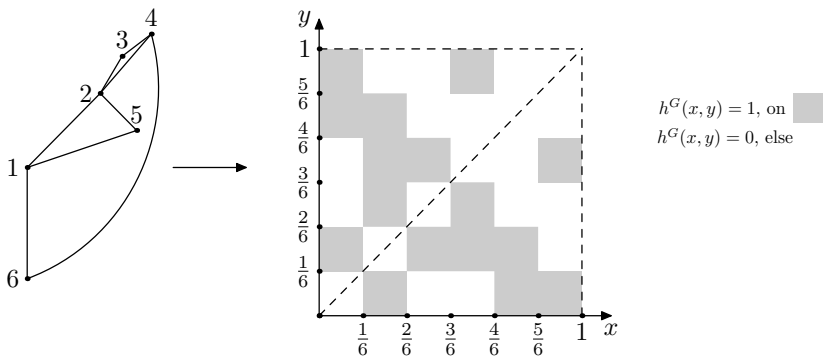

Figure 1: An example of a graph G and its graphon representation h^G.

As noted above, we suppress the n-dependence. Thus, by G we denote any simple graph on n vertices, by h^G its image in the graphon space W, and by $\tilde{h}^G$ its image in the quotient space $\tilde{W}$. For a more detailed description of the structure of the space $(\tilde{W}, \delta_\square)$ we refer the reader to [4], [5], [11]. In the sequel we will deal with constraints on the edge and triangle density. In the space W the edge density and the triangle density of a graphon h are defined by

$$T_1(h) = \int_{[0,1]^2} \mathrm{d}x_1 \mathrm{d}x_2 \, h(x_1, x_2), \quad T_2(h) = \int_{[0,1]^3} \mathrm{d}x_1 \mathrm{d}x_2 \mathrm{d}x_3 \, h(x_1, x_2) h(x_2, x_3) h(x_3, x_1). \tag{2.14}$$

For an element $\tilde{h}$ of the quotient space $\tilde{W}$ we define the edge and triangle density by

$$T_1(\tilde{h}) = T_1(h), \quad \text{and} \quad T_2(\tilde{h}) = T_2(h),$$

where h is any representative element of the equivalence class $\tilde{h}$.

2.3 Subgraph counts

Label the simple graphs in any order, e.g., F_1 is an edge, F_2 is a wedge, F_3 is triangle, etc. Let $C_k(G)$ denote the number of subgraphs F_k in G. In the dense regime, $C_k(G)$ grows like n^{V_k}, where $V_k = |V(F_k)|$ is the number of vertices in F_k. For $m \in \mathbb{N}$, consider the following *scaled vector-valued function* on $\mathcal{G}_n$:

$$\vec{C}(G) := \left(\frac{p(F_k) C_k(G)}{n^{V_k - 2}} \right)_{k=1}^m = n^2 \left(\frac{p(F_k) C_k(G)}{n^{V_k}} \right)_{k=1}^m . \tag{2.15}$$

The term $p(F_k)$ counts the edge-preserving permutations of the vertices of F_k, i.e., $p(F_1) = 2$ for an edge, $p(F_2) = 2$ for a wedge, $p(F_3) = 6$ for a triangle, etc. The term $C_k(G)/n^{V_k}$ represents a subgraph density in the graph G. The additional n^2 guarantees that the full vector scales like n^2, the scaling of the large deviation principle for graphons in the Erdős-Rényi random graph derived in [9]. For a simple graph F_k, let $\hom(F_k, G)$ be the number of homomorphisms from F_k to G, and define the *homomorphism density* as

$$t(F_k, G) := \frac{\hom(F_k, G)}{n^{V_k}} = \frac{p(F_k) C_k(G)}{n^{V_k}}, \tag{2.16}$$

which does not distinguish between permutations of the vertices. Hence the Hamiltonian becomes

$$H(\vec{\theta}, \vec{T}(G)) = n^2 \sum_{k=1}^m \theta_k \, t(F_k, G) = n^2 (\vec{\theta} \cdot \vec{T}(G)), \qquad G \in \mathcal{G}_n, \tag{2.17}$$

where

$$\vec{T}(G) := (t(F_k, G))_{k=1}^m . \tag{2.18}$$

The canonical ensemble with parameter $\vec{\theta}$ thus takes the form

$$\mathrm{P}_{\mathrm{can}}(G \mid \vec{\theta}) := \mathrm{e}^{n^2\left[\vec{\theta}\cdot\vec{T}(G)-\psi_n(\vec{\theta})\right]}, \qquad G \in \mathcal{G}_n, \tag{2.19}$$

where ψ_n replaces the *partition function* $Z(\vec{\theta})$:

$$\psi_n(\vec{\theta}) := \frac{1}{n^2}\log \sum_{G\in\mathcal{G}_n} \mathrm{e}^{n^2(\vec{\theta}\,\cdot\,\vec{T}(G))} = \frac{1}{n^2}\log Z(\vec{\theta}). \tag{2.20}$$

In the sequel we take $\vec{\theta}$ equal to a specific value $\vec{\theta}^*$, so as to meet the soft constraint, i.e.,

$$\langle \vec{T} \rangle = \sum_{G\in\mathcal{G}_n} \vec{T}(G)\,\mathrm{P}_{\mathrm{can}}(G) = \vec{T}^*. \tag{2.21}$$

The canonical probability then becomes

$$\mathrm{P}_{\mathrm{can}}(G) = \mathrm{P}_{\mathrm{can}}(G \mid \vec{\theta}^*). \tag{2.22}$$

Both the constraint $\vec{T}^*$ and the Lagrange multiplier $\vec{\theta}^*$ in general depend on n, i.e., $\vec{T}^* = \vec{T}^*_n$ and $\vec{\theta}^* = \vec{\theta}^*_n$. We consider constraints that converge when we pass to the limit $n \to \infty$, i.e.,

$$\lim_{n\to\infty} \vec{T}^*_n = \vec{T}^*_\infty. \tag{2.23}$$

Consequently, we expect that

$$\lim_{n\to\infty} \vec{\theta}^*_n = \vec{\theta}^*_\infty. \tag{2.24}$$

Throughout the sequel we *assume* that (2.24) holds. If convergence fails, then we may still consider subsequential convergence. The subtleties concerning (2.24) are discussed in [15, Appendix A].

2.4 Variational characterisation of ensemble equivalence

The expression in (2.17) can be written in terms of graphons as

$$H(\vec{\theta}, \vec{T}(G)) = n^2 \sum_{k=1}^{m} \theta_k\, t(F_k, h^G). \tag{2.25}$$

With this scaling the *hard constraint* $\vec{T}^*$ has the interpretation of the *density* of an observable quantity in G, and defines a subspace of the quotient space $\tilde{W}$, which we denote by $\tilde{W}^*$, and which consists of all graphons that meet the hard constraint, i.e.,

$$\tilde{W}^* := \{\tilde{h} \in \tilde{W} \colon\ \vec{T}(h) = \vec{T}^*_\infty\}. \tag{2.26}$$

The *soft constraint* in the canonical ensemble becomes $\langle \vec{T} \rangle = \vec{T}^*$ (recall (2.5)). Recall that for $n \in \mathbb{N}$ we write $\vec{\theta}^*$ for $\vec{\theta}^*_n$.

In order to characterise the asymptotic behavior of the two ensembles, the entropy function of a Bernoulli random variable is essential. For $u \in [0,1]$ we define

$$I(u) := \tfrac{1}{2}u\log u + \tfrac{1}{2}(1-u)\log(1-u). \tag{2.27}$$

We extend the domain of this function to the graphon space W by defining

$$I(h) := \int_{[0,1]^2} \mathrm{d}x\,\mathrm{d}y\ I(h(x,y)) \tag{2.28}$$

(with the convention that $0\log 0 = 0$). On the quotient space $(\tilde{W}, \delta_\square)$ we define $I(\tilde{h}) = I(h)$, where h is any element of the equivalence class $\tilde{h}$. In order to keep the notation minimal we use $I(\cdot)$ for both (2.27) and (2.28). Depending on the argument of the function it will be clear which of the two is considered. The key result in [15] is the following variational formula for s_∞.

Theorem 2.3 [15] *Subject to* (2.21), (2.23) *and* (2.24),

$$\lim_{n\to\infty} n^{-2} S_n(\mathrm{P}_{\mathrm{mic}} \mid \mathrm{P}_{\mathrm{can}}) =: s_\infty \tag{2.29}$$

with

$$s_\infty = \sup_{\tilde{h}\in\tilde{W}} \left[\vec{\theta}^*_\infty \cdot \vec{T}(\tilde{h}) - I(\tilde{h})\right] - \sup_{\tilde{h}\in\tilde{W}^*} \left[\vec{\theta}^*_\infty \cdot \vec{T}(\tilde{h}) - I(\tilde{h})\right]. \tag{2.30}$$

Theorem 2.3 and the compactness of $\tilde{W}^*$ give us a *variational characterisation* of ensemble equivalence: $s_\infty = 0$ if and only if at least one of the maximisers of $\vec{\theta}^*_\infty \cdot \vec{T}(\tilde{h}) - I(\tilde{h})$ in $\tilde{W}$ also lies in $\tilde{W}^* \subset \tilde{W}$. Equivalently, $s_\infty = 0$ when at least one the maximisers of $\vec{\theta}^*_\infty \cdot \vec{T}(\tilde{h}) - I(\tilde{h})$ satisfies the hard constraint. Theorem 2.3 allows us to identify cases where ensemble equivalence holds ($s_\infty = 0$) or is broken ($s_\infty > 0$). In [15] a detailed analysis was given for the special case where the constraint is on the total number of edges and the total number of triangles. The analysis in [15] relied on the large deviation principle for dense Erdős-Rényi random graphs established in [9]. The function defined in (2.27) plays a crucial role and is related to the rate function of the large deviation principle.

Theorem 2.4 [15] *For the edge-triangle model,* $s_\infty = 0$ *when*

- $T_2^* = T_1^{*3}$,
- $0 < T_1^* \leq \frac{1}{2}$ *and* $T_2^* = 0$,

while $s_\infty > 0$ *when*

- $T_2^* \neq T_1^{*3}$ *and* $T_2^* \geq \frac{1}{8}$,
- $T_2^* \neq T_1^{*3}$, $0 < T_1^* \leq \frac{1}{2}$ *and* $0 < T_2^* < \frac{1}{8}$,
- (T_1^*, T_2^*) *lies on the scallopy curve in Figure* 2.

Here, T_1^*, T_2^* are in fact the limits $T_{1,\infty}^*, T_{2,\infty}^*$ in (2.23), but in order to keep the notation light we now also suppress the index ∞.

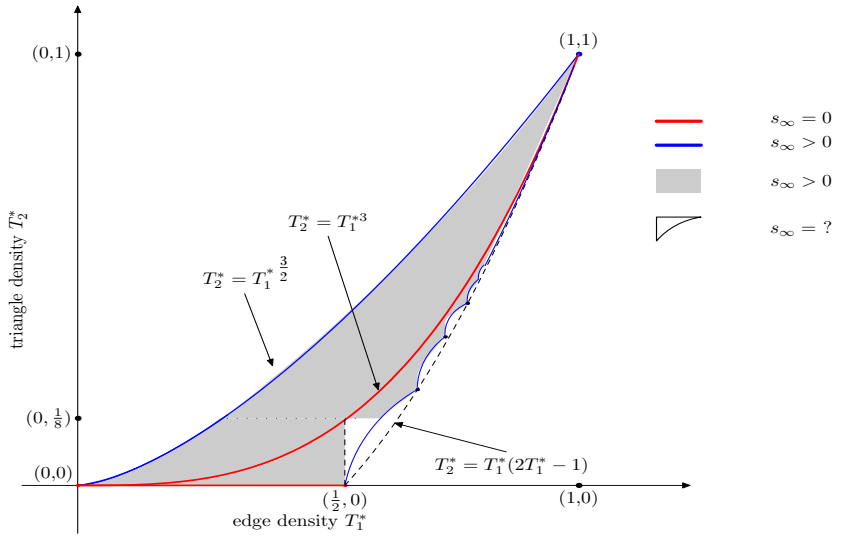

Figure 2: The admissible edge-triangle density region is the region on and between the blue curves [27].

Theorem 2.4 is illustrated in Figure 2. The region on and between the blue curves corresponds to the choices of (T_1^*, T_2^*) that are *graphical*, i.e., there exists a graph with edge density T_1^* and triangle density

T_2^*. The red curves represent ensemble equivalence, the blue curves and the grey region represent breaking of ensemble equivalence, while in the white region between the red curve and the lower blue curve we do not know what happens. Breaking of ensemble equivalence arises from *frustration*

The lower blue curve, called the *scallopy curve*, consist of infinitely many pieces labelled by $\ell \in \mathbb{N}\backslash\{1\}$. The ℓ-th piece corresponds to $T_1^* \in (\frac{\ell-1}{\ell}, \frac{\ell}{\ell+1}]$ and a T_2^* that is a function of T_1^* given by

$$T_2^* = \frac{(\ell-1)\left(\ell - 2\sqrt{\ell(\ell - T_1^*(\ell+1))}\right)\left(\ell + \sqrt{\ell(\ell - T_1^*(\ell+1))}\right)^2}{\ell^2(\ell+1)^2}. \tag{2.31}$$

We refer the reader to [24], [26], [27] and [29] for more details. The structure of the graphs drawn from the microcanonical ensemble was determined in [24] and [27]: the vertex set can be partitioned into ℓ subsets, the first $\ell-1$ subsets have size $\lfloor c_\ell n \rfloor$, the last subset has size between $\lfloor c_\ell n \rfloor$ and $2\lfloor c_\ell n \rfloor$, where

$$c_\ell := \tfrac{1}{\ell+1}\left[1 + \sqrt{1 - \tfrac{\ell+1}{\ell}\,T_1^*}\right] \in [\tfrac{1}{\ell+1}, \tfrac{1}{\ell}). \tag{2.32}$$

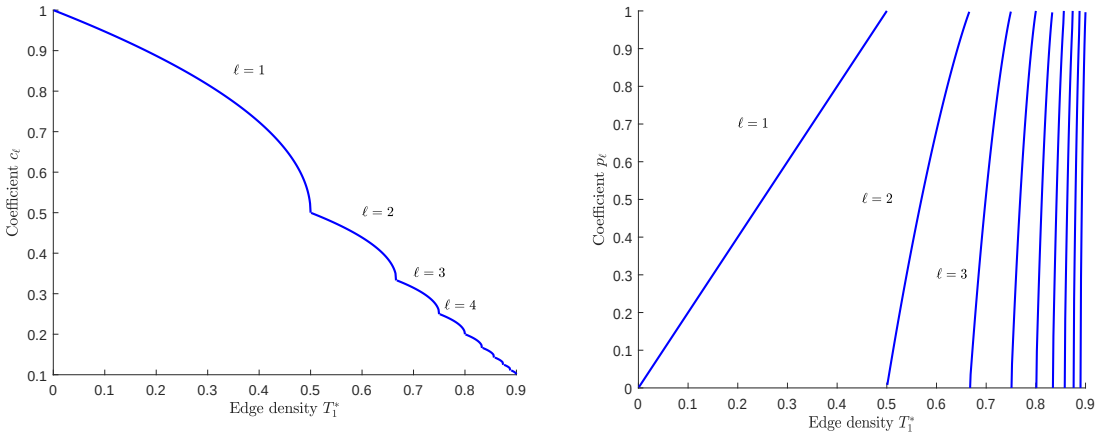

Figure 3: For $\ell \in \mathbb{N}$: c_ℓ (left) and p_ℓ (right) as a function of T_1^*.

The graph has the form of a complete ℓ-partite graph, with some additional edges on the last subset that create no triangles within that last subset. The optimal graphons have the form

$$g_\ell^*(x,y) := \begin{cases} 1, & \exists\, 1 \le k < \ell\colon\ x\ < kc_\ell <\ y \text{ or } y < kc_\ell < x, \\ p_\ell, & (\ell-1)c_\ell\ < x <\ \tfrac{1}{2}[1+(\ell-1)c_\ell] < y \text{ or } (\ell-1)c_\ell\ < y <\ \tfrac{1}{2}[1+(\ell-1)c] < x, \\ 0, & \text{otherwise}, \end{cases} \tag{2.33}$$

where

$$p_\ell = \frac{4c_\ell(1-\ell c_\ell)}{(1-(\ell-1)c_\ell)^2} \in (0,1]. \tag{2.34}$$

Figure 3 plots c_ℓ and p_ℓ as a function of T_1^* for $\ell \in \mathbb{N}$. Figure 4 is an illustration of g_ℓ^* for $\ell \in \mathbb{N}$ and $T_1^* \in (\frac{\ell-1}{\ell}, \frac{\ell}{\ell+1}]$.

3 Theorems

In this section we present our results. Our results address the following two issues:

- In Theorems 3.1–3.3 we identify the scaling behaviour of s_∞ for fixed T_1^* and $T_2^* \downarrow T_1^{*3}$, respectively, $T_2^* \uparrow T_1^{*3}$. It turns out that the way in which s_∞ tends to zero differs in the two cases.

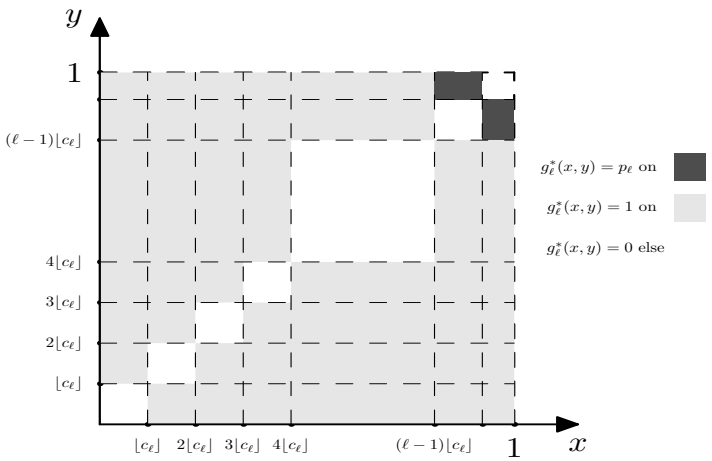

Figure 4: The graphon g_ℓ^* for $\ell \in \mathbb{N}$ and $T_1^* \in (\frac{\ell-1}{\ell}, \frac{\ell}{\ell+1}]$.

- In Theorems 3.4–3.6 we characterise the asymptotic structure of random graphs drawn from the microcanonical ensemble when the hard constraint is on the edge density and the triangle density. Our results indicate that the structure of the graphs differs in the two cases, i.e. $T_2^* \downarrow T_1^{*3}$, respectively, $T_2^* \uparrow T_1^{*3}$.

In the sequel we make the following assumption:

Assumption 1 Fix the edge density $T_1^* \in (0,1)$ and consider the triangle density $T_1^{*3} + 3T_1^*\epsilon$, for some ϵ either positive or negative. For this pair of constraints we consider the Lagrange multipliers $\vec{\theta}_\infty^*(\epsilon) := (\theta_1^*(\epsilon), \theta_2^*(\epsilon))$ as defined in Section 2.3. Then, for ϵ sufficiently small, we have the representation

$$\sup_{\tilde{h} \in \tilde{W}} \Big[\theta_1^*(\epsilon) T_1(\tilde{h}) + \theta_2^*(\epsilon) T_2(\tilde{h}) - I(\tilde{h}) \Big] = \theta_1 T_1^* - I(T_1^*) + (\gamma_1 T_1^* + \gamma_2 T_1^{*3})\epsilon + O(\epsilon^2), \tag{3.1}$$

where $\theta_1 := \theta_1(0), \gamma_1 = \theta_1'(0)$ and $\gamma_2 = \theta_2'(0)$.

In Section 4.1 we show that Assumption 1 is true when $T_1^* \in [\frac{1}{2}, 1)$. For $T_1^* \in (0, \frac{1}{2})$ we can prove (3.2) and (3.3) below but with $\geq$ replacing the equality. If Assumption 1 is true, then we again obtain (3.2) and (3.3) with equality. If it fails, then we have strict inequality.

Theorem 3.1 *For $T_1^* \in (0,1)$,*

$$\lim_{\epsilon \downarrow 0} \epsilon^{-1} s_\infty(T_1^*, T_1^{*3} + \epsilon) = \frac{1}{2T_1^*(1-T_1^*)} \in (1, \infty). \tag{3.2}$$

Theorem 3.2 *For $T_1^* \in (0, \frac{1}{2}]$,*

$$\lim_{\epsilon \downarrow 0} \epsilon^{-2/3} s_\infty(T_1^*, T_1^{*3} - \epsilon) = \tfrac{1}{2} I(2T_1^*) - I(T_1^*) \in (0, \tfrac{1}{2}\log 2]. \tag{3.3}$$

Theorem 3.3 *For $\ell \in \mathbb{N}/\{1\}$ and $T_1^* \in (\frac{\ell-1}{\ell}, \frac{\ell}{\ell+1}]$,*

$$\lim_{\epsilon \downarrow 0} \epsilon^{-2/3} s_\infty(T_1^*, T_1^{*3} - \epsilon) = \tfrac{1}{2}(1 - (\ell-1)c_\ell) I(p_\ell) - I(T_1^*) \in (0, \tfrac{1}{2}\log 2). \tag{3.4}$$

We illustrate these results in Figure 5 below. In the left panel we plot the limits in the right-hand side of (3.3)–(3.4) as a function of T_1^*. In the right panel we plot $s_\infty(T_1^*, T_1^{*3} + \epsilon)$ as function of ϵ, for ϵ sufficiently small, and for four different values of T_1^*.

In Theorems 3.4–3.6 below we identify the structure of the graphons corresponding to the perturbed constraints in the microcanonical ensemble in the limit as $n \to \infty$.

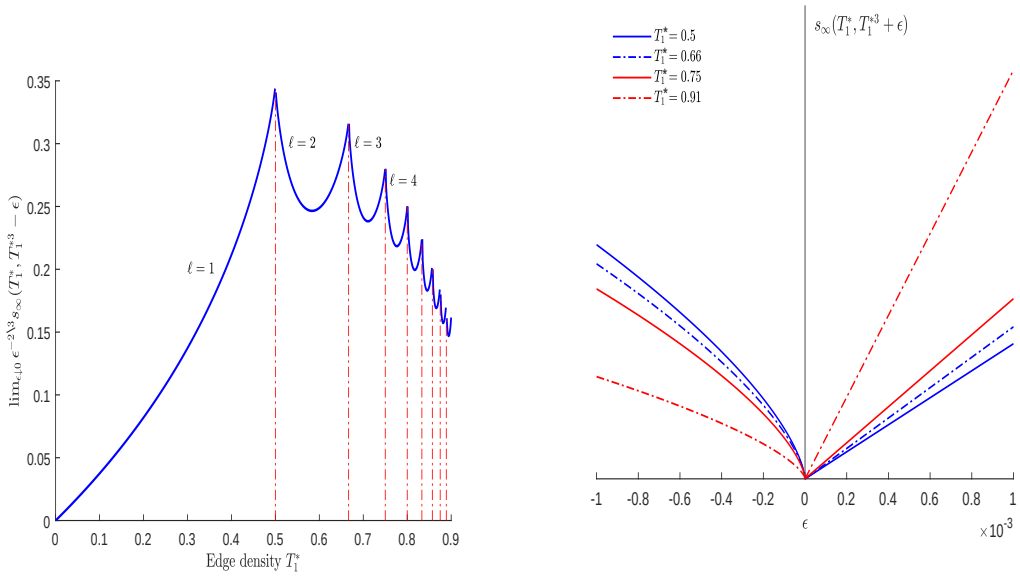

Figure 5: Limit of scaled s_∞ as a function of $T_1^* \in (0,1)$ (left panel) and of s_∞ as a function of ϵ for ϵ sufficiently small (right panel).

Theorem 3.4 *When the ER-line is approached from above, the optimal perturbation of the graphon is*

$$h = T_1^* + \sqrt{\epsilon}\, g^* + O(\epsilon) \qquad \text{(global perturbation)} \tag{3.5}$$

with g^* the graphon

$$g^*(x,y) = \begin{cases} 2, & (x,y) \in [0,\frac{1}{2}]^2, \\ 0, & (x,y) \in [0,\frac{1}{2}] \times (\frac{1}{2},1] \cup (\frac{1}{2},1] \times [0,\frac{1}{2}], \\ -2, & (x,y) \in (\frac{1}{2},1]^2. \end{cases} \tag{3.6}$$

Theorem 3.5 *When the ER-line is approached from below and $T_1^* \in (0,\frac{1}{2}]$, the optimal perturbation is*

$$h = T_1^*\, 1_{[0,1]^2 \setminus \square_\epsilon} + g^*_{\square_{\epsilon'}} \qquad \text{(local perturbation)} \tag{3.7}$$

with $\square_{\epsilon'} = [0,\epsilon'^{1/3}]^2$, $\epsilon' = \epsilon + O(\epsilon^{4/3})$ and $g^*_{\square_{\epsilon'}}$ the graphon

$$g^*_{\square_{\epsilon'}}(x,y) := \begin{cases} 2T_1^*, & 0 < x < \frac{1}{2}\epsilon'^{1/3} < y < \epsilon'^{1/3} \text{ or } 0 < y < \frac{1}{2}\epsilon'^{1/3} < x < \epsilon'^{1/3}, \\ 0, & \text{otherwise.} \end{cases} \tag{3.8}$$

Theorem 3.6 *When the ER-line is approached from below and $T_1^* \in (\frac{\ell-1}{\ell}, \frac{\ell}{\ell+1}]$, $\ell \in \mathbb{N}/\{1\}$, the optimal perturbation is*

$$h = T_1^*\, 1_{[0,1]^2 \setminus \square_{\epsilon'}} + g^*_{\square_{\epsilon'}} \qquad \text{(local perturbation)} \tag{3.9}$$

with $\square_{\epsilon'} = [0,\epsilon'^{1/3}]^2$, $\epsilon' = \epsilon + O(\epsilon^{4/3})$ and $g^*_{\square_{\epsilon'}}$ the graphon

$$g^*_{\square_{\epsilon'}}(x,y) := \begin{cases} 1, & \exists\, 1 \le k < \ell\colon\ x < kc_\ell\epsilon'^{1/3} < y \text{ or } y < kc_\ell\epsilon'^{1/3} < x, \\ p_\ell, & (\ell-1)c_\ell\epsilon'^{1/3} < x < \frac{1}{2}[1+(\ell-1)c_\ell]\epsilon'^{1/3} < y < \epsilon'^{1/3} \\ & \text{or } (\ell-1)c_\ell\epsilon'^{1/3} < y < \frac{1}{2}[1+(\ell-1)c_\ell]\epsilon'^{1/3} < x < \epsilon'^{1/3}, \\ 0, & \text{otherwise.} \end{cases} \tag{3.10}$$

The terms c_ℓ and p_ℓ were defined above in (2.32) *and* (2.34).

In conclusion, Theorems 3.1–3.3 say that at a fixed density of the edges it is less costly in terms of relative entropy to increase the density of triangles than to decrease it. The ER-line represents a crossover in the cost (see Figure 5, right panel). Above the ER-line the cost is linear in the distance, below the ER-line the cost is proportional to the $\frac{2}{3}$-power of the distance. Theorems 3.4–3.6 show that the optimal perturbation of the ER-graphon is global above the ER-line and local below the ER-line. Note that, as we move down from the ER-line to the scallopy curve in Figure 2, the optimal graphons in (3.8) and (3.10) converge to the optimal graphon in (2.33).

4 Proofs of Theorems 3.1–3.3

In this section we prove Theorems 3.1–3.3. Along the way we use the results given in Theorems 3.4–3.6, which we prove in Section 5.

4.1 Proof of Theorem 3.1

For ease of notation we drop the superscript $*$ from the constraint on the edge density and write T_1 instead of T_1^*. Let

$$T_1(\epsilon) = T_1, \qquad T_2(\epsilon) = T_1^3 + 3T_1\epsilon. \tag{4.1}$$

The factor $3T_1$ appearing in front of the ϵ is put in for convenience. We know that for every pair of graphical constraints $(T_1(\epsilon), T_2(\epsilon))$ there exists a unique pair of Lagrange multipliers $(\theta_1(\epsilon), \theta_2(\epsilon))$ corresponding to these constraints. For an elaborate discussion on this issue we refer the reader to [15]. By considering the Taylor expansion of the Lagrange multipliers $(\theta_1(\epsilon), \theta_2(\epsilon))$ around $\epsilon = 0$, we obtain

$$\theta_1(\epsilon) = \theta_1 + \gamma_1\epsilon + \tfrac{1}{2}\Gamma_1\epsilon^2 + O(\epsilon^3), \qquad \theta_2(\epsilon) = \gamma_2\epsilon + \tfrac{1}{2}\Gamma_2\epsilon^2 + O(\epsilon^3), \tag{4.2}$$

where

$$\theta_1(0) = \theta_1 = I'(T_1), \qquad \gamma_1 = \theta_1'(0), \qquad \Gamma_1 = \theta_1''(0), \qquad \theta_2(0) = 0, \qquad \gamma_2 = \theta_2'(0), \qquad \Gamma_2 = \theta_2''(0). \tag{4.3}$$

We denote the two terms in the expression for s_∞ in (2.30) by I_1, I_2, i.e.,

$$s_\infty = \sup_{\tilde{h}\in\tilde{W}} \left[\vec{\theta}_\infty \cdot \vec{T}(\tilde{h}) - I(\tilde{h})\right] - \sup_{\tilde{h}\in\tilde{W}^*} \left[\vec{\theta}_\infty \cdot \vec{T}(\tilde{h}) - I(\tilde{h})\right] = I_1 - I_2, \tag{4.4}$$

and we let $s_\infty(\epsilon)$ denote the relative entropy corresponding to the perturbed constraints. We distinguish between the cases $T_1 \in [\frac{1}{2}, 1)$ and $T_1 \in (0, \frac{1}{2})$.

Case I $T_1 \in [\frac{1}{2}, 1)$**:** From [15, Section 5], if $T_1 \in [\frac{1}{2}, 1)$ and $T_2 \in [\frac{1}{8}, 1)$, then the corresponding Lagrange multipliers (θ_1, θ_2) are both non-negative. Hence from [7, Theorem 4.1] we have that

$$I_1 := \sup_{\tilde{h}\in\tilde{W}} \left[\theta_1(\epsilon)T_1(\tilde{h}) + \theta_2(\epsilon)T_2(\tilde{h}) - I(\tilde{h})\right] = \sup_{0\le u\le 1} \left[\theta_1(\epsilon)u + \theta_2(\epsilon)u^2 - I(u)\right], \tag{4.5}$$

and, consequently,

$$I_1 = \sup_{0<u<1} \left[\theta_1(\epsilon)u + \theta_2(\epsilon)u^3 - I(u)\right] = \theta_1(\epsilon)u^*(\epsilon) + \theta_2(\epsilon)u^*(\epsilon)^3 - I(u^*(\epsilon)). \tag{4.6}$$

The optimiser $u^*(\epsilon)$ corresponding to the perturbed multipliers $\theta_1^*(\epsilon)$ and $\theta_2^*(\epsilon)$ is analytic in ϵ, as shown in [28]. Therefore, a Taylor expansion around $\epsilon = 0$ gives

$$u^*(\epsilon) = T_1 + \delta\epsilon + \tfrac{1}{2}\Delta\epsilon^2 + O(\epsilon^3), \tag{4.7}$$

where $\delta = u^{*\prime}(0)$ and $\Delta = u^{*\prime\prime}(0)$. Hence I_1 can be written as

$$I_1 = \theta_1 T_1 - I(T_1) + (\gamma_1 T_1 + \gamma_2 T_1^3)\epsilon + O(\epsilon^2). \tag{4.8}$$

Moreover,

$$\begin{aligned} I_2 &= \big[\theta_1 + \gamma_1\epsilon + \tfrac{1}{2}\Gamma_1\epsilon^2 + O(\epsilon^3)\big]T_1 + \big[\gamma_2\epsilon + \tfrac{1}{2}\Gamma_2\epsilon^2 + O(\epsilon^3)\big](T_1^3 + 3T_1\epsilon) - \inf_{\tilde{h}\in\tilde{W}_\epsilon^*} I(\tilde{h}) \\ &= \theta_1 T_1 + \gamma_1 T_1\epsilon + \tfrac{1}{2}\Gamma_1 T_1\epsilon^2 + T_1^3\gamma_2\epsilon + \tfrac{1}{2}\Gamma_2 T_1^3\epsilon^2 + 3T_1\gamma_2\epsilon^2 - J^{\downarrow}(\epsilon) + O(\epsilon^3), \end{aligned} \tag{4.9}$$

where

$$J^{\downarrow}(\epsilon) := \inf_{\tilde{h}\in\tilde{W}_\epsilon^*} I(\tilde{h}), \qquad \tilde{W}_\epsilon^* := \{\tilde{h}\in\tilde{W}\colon\ T_1(\tilde{h}) = T_1,\ T_2(\tilde{h}) = T_1^3 + 3T_1\epsilon\}. \tag{4.10}$$

Consequently,

$$s_\infty(\epsilon) = J^{\downarrow}(\epsilon) - I(T_1) + O(\epsilon^2). \tag{4.11}$$

Denote by $\tilde{h}_\epsilon^*$ one of the, possibly multiple, optimisers of the variational problem $J^{\downarrow}(\epsilon)$. From Theorem 3.4 we know that any graphon, denoted by h_ϵ^* for simplicity in the notation, in the equivalence class $\tilde{h}_\epsilon^*$ has the form $h_\epsilon^* = T_1 + \sqrt{\epsilon}g + O(\epsilon)$ for some function $g\in U$, where

$$U := \left\{ g\colon\ [0,1]^2\to\mathbb{R},\ g \text{ symmetric},\ \int_{[0,1]^2} \mathrm{d}x\ \mathrm{d}y\ g(x,y) = 0,\ \ \int_{[0,1]^3} \mathrm{d}x\ \mathrm{d}y\ \mathrm{d}z\ g(x,y)g(y,z) = 1 \right\}. \tag{4.12}$$

By considering the Taylor expansion of the function I around $\epsilon = 0$, we get

$$\begin{aligned} J^{\downarrow}(\epsilon) &= I(T_1) + I'(T_1)\sqrt{\epsilon}\inf_{g\in U}\left(\int_{[0,1]^2}\mathrm{d}x\,\mathrm{d}y\,g(x,y)\right) + \tfrac{1}{2}I''(T_1)\,\epsilon\inf_{g\in U}\left(\int_{[0,1]^2}\mathrm{d}x\,\mathrm{d}y\,g(x,y)^2\right) + o(\epsilon) \\ &= I(T_1) + \tfrac{1}{2}I''(T_1)\,\epsilon\inf_{g\in U}\left(\int_{[0,1]^2}\mathrm{d}x\,\mathrm{d}y\,g(x,y)^2\right) + o(\epsilon) \\ &= I(T_1) + \tfrac{1}{2}I''(T_1)V + o(\epsilon), \end{aligned} \tag{4.13}$$

where

$$V = \inf_{g\in U}\left(\int_{[0,1]^2}\mathrm{d}x\,\mathrm{d}y\,g(x,y)^2\right), \tag{4.14}$$

Hence we obtain

$$s_\infty(\epsilon) = K^{\downarrow}(T_1)\,\epsilon + o(\epsilon) \tag{4.15}$$

with

$$K^{\downarrow}(T_1) = \tfrac{1}{2}I''(T_1)V = \frac{1}{4}\frac{V}{T_1(1-T_1)} > 0. \tag{4.16}$$

At the end of Section 5.1, in (5.51), we show that $V = 2$. Hence we have that $K^{\downarrow}(T_1) = I''(T_1) = \frac{1}{2}\frac{1}{T_1(1-T_1)}$.

Case II $T_1\in(0,\frac{1}{2})$**:** Consider the term $I_1 := \sup_{\tilde{h}\in\tilde{W}}\left[\theta_1(\epsilon)T_1(\tilde{h}) + \theta_2(\epsilon)T_2(\tilde{h}) - I(\tilde{h})\right]$, as above. If Assumption 1 applies, then this case is proved in the same way as Case I. Otherwise, consider the following straightforward lower bound

$$\sup_{\tilde{h}\in\tilde{W}}\left[\theta_1(\epsilon)T_1(\tilde{h}) + \theta_2(\epsilon)T_2(\tilde{h}) - I(\tilde{h})\right] \geq \sup_{0\leq u\leq 1}\left[\theta_1(\epsilon)u + \theta_2(\epsilon)u^3 - I(u)\right]. \tag{4.17}$$

The arguments used in Case I after (4.6) apply, and the result in (4.11) is obtained with an inequality instead of an equality.

4.2 Proof of Theorem 3.2

In this section we omit the computations that are similar to those in the proof of Theorem 3.1 in Section 4.1. Let

$$T_1(\epsilon) = T_1, \qquad T_2(\epsilon) = T_1^3 - T_1^3\ \epsilon. \tag{4.18}$$

The perturbed Lagrange multipliers are

$$\theta_1(\epsilon) = \theta_1 + \gamma_1\epsilon + \tfrac{1}{2}\Gamma_1\epsilon^2 + O(\epsilon^3), \qquad \theta_2(\epsilon) = \gamma_2\epsilon + \tfrac{1}{2}\Gamma_2\epsilon^2 + O(\epsilon^3), \tag{4.19}$$

where

$$\theta_1 = I'(T_1), \qquad \gamma_1 = \theta_1'(0), \qquad \Gamma_1 = \theta_1''(0) \qquad \gamma_2 = \theta_2'(0), \qquad \Gamma_2 = \theta_2''(0). \tag{4.20}$$

We denote the two terms in the expression for s_∞ in (2.30) by I_1, I_2, i.e., $s_\infty = I_1 - I_2$, and let $s_\infty(\epsilon)$ denote the perturbed relative entropy. The computations for I_1 are similar as before, because the exact form of the constraint does not affect the expansions in (4.7) and (4.8). For I_2, on the other hand, we have

$$\begin{aligned} I_2 &= \theta_1 T_1 + \gamma_1 T_1\epsilon + \tfrac{1}{2}\Gamma_1 T_1\epsilon^2 + T_1^3\gamma_2\epsilon + \tfrac{1}{2}\Gamma_2 T_1^3\epsilon^2 - T_1^3\gamma_2\epsilon^2 - J_1^{\uparrow}(\epsilon) \\ &= \theta_1 T_1 + \gamma_1 T_1\epsilon + T_1^3\gamma_2\epsilon - J_1^{\uparrow}(\epsilon) + O(\epsilon^2), \end{aligned} \tag{4.21}$$

where

$$J_1^{\uparrow}(\epsilon) := \inf_{\tilde{h}\in\tilde{W}_\epsilon^*} I(\tilde{h}), \qquad \tilde{W}_\epsilon^* := \{\tilde{h}\in\tilde{W}\colon\ T_1(\tilde{h}) = T_1,\ T_2(\tilde{h}) = T_1^3 - T_1^3\ \epsilon\}. \tag{4.22}$$

Consequently,

$$s_\infty(\epsilon) = J_1^{\uparrow}(\epsilon) - I(T_1) + O(\epsilon^2). \tag{4.23}$$

Denote by $\tilde{h}_\epsilon^*$ one of the, possibly multiple, optimisers of the variational problem $J^{\uparrow}(\epsilon)$. From Theorem 3.5 we know that, for $T_1 \in (0, \frac{1}{2}]$, any graphon, denoted by h_ϵ^* for simplicity in the notation, in the equivalence class $\tilde{h}_\epsilon^*$ has the form

$$h_\epsilon^* = T_1\, 1_{[0,1]^2\setminus\square_{\epsilon'}} + \bar{g}^*_{\square_{\epsilon'}} \tag{4.24}$$

with $\square_{\epsilon'} = [0, \epsilon'^{1/3}]^2$, $\epsilon' = \epsilon + O(\epsilon^{4/3})$ and $\bar{g}^*_{\square_{\epsilon'}}$ the graphon

$$g^*_{\square_{\epsilon'}}(x,y) := \begin{cases} 2T_1^*, & 0 < x < \frac{1}{2}\epsilon'^{1/3} < y < \epsilon'^{1/3} \text{ or } 0 < y < \frac{1}{2}\epsilon'^{1/3} < x < \epsilon'^{1/3}, \\ 0 & \text{otherwise.} \end{cases} \tag{4.25}$$

Hence

$$J_1^{\uparrow}(\epsilon) = I(T_1) + \epsilon^{2/3}\left(\tfrac{1}{2}I(2T_1) - I(T_1)\right) = I(T_1) + K_1^{\uparrow}(T_1)\epsilon^{2/3}, \tag{4.26}$$

which gives

$$s_\infty(\epsilon) = K_1^{\uparrow}(T_1)\epsilon^{2/3} + o(\epsilon^{2/3}), \tag{4.27}$$

where $K_1^{\uparrow}(T_1) := \frac{1}{2}I(2T_1) - I(T_1)$. The latter is larger than zero because I is convex and $I(0) = I(1) = 0$.

4.3 Proof of Theorem 3.3

The computations leading to the expression for the relative entropy in the right-hand side of (3.4) are similar as those in Section 4.2, and we omit them. Hence we have

$$s_\infty(\epsilon) = J_\ell^{\uparrow}(\epsilon) - I(T_1) + O(\epsilon^2), \tag{4.28}$$

where, for $\ell \in \mathbb{N}\setminus\{1\}$ and $T_1 \in (\frac{\ell-1}{\ell}, \frac{\ell}{\ell+1}]$,

$$J_\ell^{\uparrow}(\epsilon) := \inf_{\tilde{h}\in\tilde{W}_\epsilon^*} I(\tilde{h}), \qquad \tilde{W}_\epsilon^* := \{\tilde{h}\in\tilde{W} : T_1(\tilde{h}) = T_1,\ T_2(\tilde{h}) = T_1^3 - T_1^3\ \epsilon\}. \tag{4.29}$$

In this case the optimal perturbation depends on the value of ℓ. We observe that the construction in (4.25) is not possible for $T_1 \in (\frac{1}{2}, 1]$. This is because a bipartite graph has maximum edge density

equal to $\frac{1}{2}$. From Theorem 3.6 and after a straightforward computation we get that the first term in the right-hand side of (3.4) corresponds to the entropy of the graphon given in (3.10). In what follows we prove that the right-hand side of (3.10) is positive. We consider, for $\ell \in \mathbb{N}$ and $T_1 \in (\frac{\ell-1}{\ell}, \frac{\ell}{\ell+1}]$, the function

$$L_\ell(T_1) = \tfrac{1}{2}(1-(\ell-1)c_\ell)I(p_\ell), \tag{4.30}$$

where c_ℓ and p_ℓ are defined in (2.32) and (2.34), and depend on T_1 (we suppress this dependence from the notation). In what follows we prove that, for every $\ell \in \mathbb{N}\setminus\{1\}$ and $T_1 \in (\frac{\ell-1}{\ell}, \frac{\ell}{\ell+1}]$,

$$L_\ell(T_1) = \tfrac{1}{2}(1-(\ell-1)c_\ell)I(p_\ell) > I(T_1). \tag{4.31}$$

In the proof we will need the following lemma.

Lemma 4.1 *For every $\ell \in \mathbb{N}$, p_ℓ as a function of T_1 is increasing and concave on the interval $(\frac{\ell-1}{\ell}, \frac{\ell}{\ell+1}]$, and maps this interval to $(0,1]$.*

Proof. From (2.34) we have that

$$p_\ell = \frac{4c_\ell(1-\ell c_\ell)}{(1-(\ell-1)c_\ell)^2}, \tag{4.32}$$

where c_ℓ is defined in (2.32). A straightforward computation shows that, for $T_1 = \frac{\ell-1}{\ell}$, $c_\ell = \frac{1}{\ell}$ and $p_\ell = 0$. Similarly, for $T_1 = \frac{\ell}{\ell+1}$, $c_\ell = \frac{1}{\ell+1}$ and $p_\ell = 1$. Computing the derivative of p_ℓ with respect to T_1, we obtain

$$p'_\ell = \frac{4c'_\ell(1-c_\ell(\ell+1))}{(1-(\ell-1)c_\ell)^3} \quad \text{with} \quad c'_\ell = -\frac{1}{2\ell}\frac{1}{\sqrt{1-\frac{\ell+1}{\ell}T_1}}. \tag{4.33}$$

Substituting c'_ℓ into the expression for p'_ℓ, we obtain

$$p'_\ell = \frac{2}{\ell}\frac{1}{(1-(\ell-1)c_\ell)^3}. \tag{4.34}$$

Observe that $c'_\ell < 0$. From (2.32) we get that $c_\ell \in (\frac{1}{\ell+1}, \frac{1}{\ell}]$. Thus, from (4.34) we get that $p'_\ell > 0$ on every interval $(\frac{\ell-1}{\ell}, \frac{\ell}{\ell+1}]$ (see Figure 3). A straightforward computation from (4.34) shows that

$$p''_\ell = -\frac{6(\ell-1)}{\ell}\frac{c'_\ell}{(1-(\ell-1)c_\ell)^5} < 0. \tag{4.35}$$

∎

From Lemma 4.1 we see that p_ℓ is a one-to-one mapping of the interval $(\frac{\ell-1}{\ell}, \frac{\ell}{\ell+1}]$ to $(0,1]$. Hence there is a unique $\tilde{T}_1 \in (\frac{\ell-1}{\ell}, \frac{\ell}{\ell+1}]$ at which $I(p_\ell(\tilde{T}_1))$ is minimised, namely, the unique solution of the equation $p_\ell = \frac{1}{2}$ on $(\frac{\ell-1}{\ell}, \frac{\ell}{\ell+1}]$. Existence and uniqueness of this solution follows from Lemma 4.1. Moreover, $I(p_\ell(\tilde{T}_1)) = \frac{1}{2}\log\frac{1}{2}$. The function L_ℓ in (4.31) is just a rescaling of $I(p_\ell)$ on the interval $(\frac{\ell-1}{\ell}, \frac{\ell}{\ell+1}]$. The scaling is due to the multiplication by the factor $\frac{1}{2}(1-(\ell-1)c_\ell)$, where $\frac{1}{2}(1-(\ell-1)c_\ell) \in (\frac{1}{2\ell}, \frac{1}{\ell+1})$. Hence, for every $\ell \in \mathbb{N}$ and every $T_1 \in (\frac{\ell-1}{\ell}, \frac{\ell}{\ell+1}]$,

$$L_\ell(T_1) > \frac{1}{\ell+1}I(p_\ell). \tag{4.36}$$

Therefore it suffices to show that, for every $\ell \in \mathbb{N}$ and every $T_1 \in (\frac{\ell-1}{\ell}, \frac{\ell}{\ell+1}]$,

$$\frac{1}{\ell+1}I(p_\ell) > I(T_1). \tag{4.37}$$

On the interval $(\frac{\ell-1}{\ell}, \frac{\ell}{\ell+1}]$ the function $\frac{1}{\ell+1}I(p_\ell)$ attains a minimum at the unique point $\tilde{T}_1$ where $p_\ell(\tilde{T}_1) = \frac{1}{2}$, with minimum value equal to $\frac{1}{\ell+1}I(\frac{1}{2})$. On the same interval the function I is increasing

because $\ell \in \mathbb{N} \setminus \{1\}$, and attains its maximum value at $T_1 = \frac{\ell}{\ell+1}$. Hence it suffices to show that, for every $\ell \in \mathbb{N} \setminus \{1\}$,

$$I\left(\tfrac{1}{2}\right) > (\ell+1) I\left(\tfrac{\ell}{\ell+1}\right). \tag{4.38}$$

The function $(x+1)I\left(\frac{x}{1+x}\right)$, $x \geq 1$, is decreasing because

$$\left((1+x)I\left(\frac{x}{1+x}\right)\right)' = I\left(\frac{x}{1+x}\right) + \frac{1}{1+x} I'\left(\frac{x}{1+x}\right) = \log \frac{x}{1+x} < 0. \tag{4.39}$$

Thus, $(x+1)I(\frac{x}{1+x}) < 2I(\frac{1}{2}) < I(\frac{1}{2})$, $x > 1$, which proves (4.38) and consequently also (4.30).

5 Proofs of Theorems 3.4–3.6

In this section we prove Theorems 3.4 - 3.6. In Section 5.1 we prove Theorem 3.4 and in Section 5.2 we prove Theorem 3.5. The proof of Theorem 3.6 is similar to the proof of Theorem 3.5, just the computations are slightly more involved. We include a discussion on how to extend the proof of Theorem 3.5 for this case in Section 5.2.

As we have already seen in Section 4, the following variational problems were encountered:

(1) For $T_1 \in (0,1)$,

$$J^{\downarrow}(\epsilon) = \inf\left\{I(\tilde{h})\colon\ \tilde{h} \in \tilde{W},\, T_1(\tilde{h}) = T_1,\, T_2(\tilde{h}) = T_1^3 + 3T_1\epsilon\right\}. \tag{5.1}$$

(2) For $T_1 \in (0, \frac{1}{2}]$

$$J_1^{\uparrow}(\epsilon) = \inf\left\{I(\tilde{h})\colon\ \tilde{h} \in \tilde{W},\, T_1(\tilde{h}) = T_1,\, T_2(\tilde{h}) = T_1^3 - T_1^3\epsilon\right\}. \tag{5.2}$$

(3) For $T_1 \in [\frac{\ell-1}{\ell}, \frac{\ell}{\ell+1}]$, $\ell \in \mathbb{N}/\{1\}$,

$$J_\ell^{\uparrow}(\epsilon) = \inf\left\{I(\tilde{h})\colon\ \tilde{h} \in \tilde{W},\, T_1(\tilde{h}) = T_1,\, T_2(\tilde{h}) = T_1^3 - T_1^3\epsilon\right\}. \tag{5.3}$$

In order to prove Theorems 3.4–3.6, we need to analyse these three variational problems, for ϵ sufficiently small, which is the objective of this section. We analyse these variational expressions with the help of a perturbation argument. In particular, we show that the optimal perturbations are those given in (3.5), (3.7) and (3.9), respectively. We summarise the results in the following three lemmas. The results in Theorems 3.4–3.6 follow directly from these lemmas.

Lemma 5.1 *Let $T_1 \in (0,1)$. For $\epsilon > 0$ consider the variational problem $J^{\downarrow}(\epsilon)$ given in (5.1). Then, for ϵ sufficiently small,*

$$J^{\downarrow}(\epsilon) = I(T_1) + I''(T_1)\epsilon + o(\epsilon), \tag{5.4}$$

Lemma 5.2 *Let $T_1 \in (0, \frac{1}{2}]$. For $\epsilon > 0$ consider the variational problem $J_1^{\uparrow}(\epsilon)$ given in (5.2). Then, for ϵ sufficiently small,*

$$J_1^{\uparrow}(\epsilon) = I(T_1) + \epsilon^{2/3}\left(\tfrac{1}{2} I(2T_1) - I(T_1)\right). \tag{5.5}$$

Lemma 5.3 *Consider an $\ell \in \mathbb{N}\backslash\{1\}$ and let $T_1 \in (\frac{\ell-1}{\ell}, \frac{\ell}{\ell+1}]$. For $\epsilon > 0$ consider the variational problem $J_\ell^{\uparrow}(\epsilon)$ given in (5.3). Then, for ϵ sufficiently small,*

$$J_\ell^{\uparrow}(\epsilon) = I(T_1) + \epsilon^{2/3}\left(\tfrac{1}{2}(1-(\ell-1)c_\ell I(p_\ell) - I(T_1)\right), \tag{5.6}$$

where c_ℓ and p_ℓ are functions of T_1 defined in (2.32) and (2.34), respectively.

In what follows we use the notation $f(\epsilon) \asymp g(\epsilon)$, for two functions f, g, when $\frac{f(\epsilon)}{g(\epsilon)}$ converges to a *positive* constant, as $\epsilon \downarrow 0$.

5.1 Proof of Lemma 5.1

In this section we prove Lemma 5.1. Before presenting the technical details of the proof we first explain how Theorem 3.4 follows from Lemma 5.1. Afterwards, we intuitively explain why the results in Theorem 3.4 and Lemma 5.1 are true. In order to find the optimal perturbation when the ER-line is approached from above we need to solve $J^{\downarrow}(\epsilon)$ in (5.1). From Lemma 5.1 we get that the optimiser lies in a the smaller class of graphons, those having the form given in (3.5). The following construction, which is not necessarily the optimal one, shows intuitively why the optimal perturbation has the form in (3.5). Consider the following inhomogeneous ER-random graph on n vertices. We split the vertices of the graph into two parts of equal size, that is of size $n/2$. In one part we connect two vertices with probability $T_1 + 2\sqrt{\epsilon}$, in the second part we connect two vertices with probability $T_1 - 2\sqrt{\epsilon}$ and we connect vertices lying in different parts with probability T_1. This graph has expected edge density equal to

$$\frac{1}{\binom{n}{2}}\left(T_1(\frac{n}{2})^2 + (T_1+2\sqrt{\epsilon})\binom{\frac{n}{2}}{2} + (T_1-2\sqrt{\epsilon})\binom{\frac{n}{2}}{2}\right) = T_1. \tag{5.7}$$

Similarly, the expexted triangle density is equal to

$$\frac{1}{\binom{n}{3}}\frac{1}{8}\left((T_1+2\sqrt{\epsilon})^3 + 3T_1^2(T_1+2\sqrt{\epsilon}) + 3T_1^2(T_1-2\sqrt{\epsilon}) + (T_1-2\sqrt{\epsilon})^3\right) = T_1^3 + 3T_1\epsilon. \tag{5.8}$$

In the proof below we will see that the optimal perturbation is indeed given by the graphon counterpart of the inhomogeneous ER-random graph described above. We now proceed to write out the technical details of the proof.

Our argument relies only on the strict convexity of the function $I(\cdot)$, defined in (2.27). With a slight abuse of notation we write $I(\cdot)$ for both cases of a graphon and a real number. We consider the variational problem $J^{\downarrow}(\epsilon)$ for $\epsilon > 0$ as given in (5.1). We denote by $\tilde{h}_\epsilon^{*\downarrow}$ one of the, possibly multiple, optimisers of $J^{\downarrow}(\epsilon)$. For simplicity in the notation, in what follows, we work with a representative element, denoted by $h_\epsilon^{*\downarrow}$, of the equivalence class $\tilde{h}_\epsilon^{*\downarrow}$. We write the optimiser $h_\epsilon^{*\downarrow}$ in the form $h_\epsilon^{*\downarrow} = T_1 + \Delta H_\epsilon$ for some bounded symmetric function ΔH_ϵ defined on the unit square $[0,1]^2$ and taking values in $\mathbb{R}$. This term will be called the *perturbation term*. The optimiser $h_\epsilon^{*\downarrow}$ has to satisfy the conditions on the edge and triangle densities, i.e.,

$$T_1(h_\epsilon^{*\downarrow}) = T_1 \qquad \text{and} \qquad T_2(h_\epsilon^{*\downarrow}) = T_1^3 + 3T_1\epsilon. \tag{5.9}$$

Hence the perturbation term ΔH_ϵ needs to satisfy the following two constraints

$$(G_1)\colon \quad \int_{[0,1]^2} \mathrm{d}x\,\mathrm{d}y\ \Delta H_\epsilon(x,y) = 0, \tag{5.10}$$

and

$$\begin{aligned}(G_2)\colon\ 3T_1 &\int_{[0,1]^3} \mathrm{d}x\,\mathrm{d}y\,\mathrm{d}z\ \ \Delta H_\epsilon(x,y)\Delta H_\epsilon(y,z) \\ &+ \int_{[0,1]^3} \mathrm{d}x\,\mathrm{d}y\,\mathrm{d}z\ \ \Delta H_\epsilon(x,y)\Delta H_\epsilon(y,z)\Delta H_\epsilon(z,x) = 3T_1\epsilon.\end{aligned} \tag{5.11}$$

We split the proof into two steps. In Step 1 we show that in order to solve $J^{\downarrow}(\epsilon)$ it suffices to look at graphons that are piece-wise constant functions on $[0,1]^2$ with two possible non-zero values. In Step 2 we show that it suffices to look at the variational problem given in (5.4), i.e., the optimal perturbation is a two-step function and on the order of $\sqrt{\epsilon}$. In Step 1 we do not yet take the two constraints (G_1) and (G_2) into consideration, we proof the more general result that, if we want to minimise $I(\cdot)$, we may restrict ourselves to the subclass of piece-wise constant graphons. In Step 2 we consider the class of piece-wise constant graphons satisfying the constraints.

Step 1: We show that, in order to solve the variational problem $J^{\downarrow}(\epsilon)$, it suffices to look at graphons that are piecewise constant with two non-zero steps. Such graphons correspond to inhomogeneous ER random graphs. Consider, for $\epsilon > 0$, the perturbed graphon $T_1 + \Delta H_\epsilon$, where ΔH_ϵ is a bounded symmetric function defined on $[0,1]^2$. For this function we consider the two sets

$$\begin{aligned} \mathcal{J}^+ &:= \{(x,y) \in [0,1]^2 : \ \Delta H_\epsilon(x,y) > 0\}, \\ \mathcal{J}^- &:= \{(x,y) \in [0,1]^2 : \ \Delta H_\epsilon(x,y) < 0\}, \end{aligned} \tag{5.12}$$

and suppose that $0 < \lambda(\mathcal{J}^+) < 1$. In Step 2 we will see that this condition is indeed satisfied in our setting. We consider the two-step function, denoted by ΔA_ϵ, defined on $[0,1]^2$ where the steps are the average values of ΔH_ϵ on $\mathcal{J}^+$ and $\mathcal{J}^-$, respectively, i.e.,

$$\Delta A_\epsilon = A^+ 1_{\mathcal{J}^+} + A^- 1_{\mathcal{J}^-}, \tag{5.13}$$

where

$$A^+ := \frac{1}{\lambda(\mathcal{J}^+)} \int_{\mathcal{J}^+} \mathrm{d}x\, \mathrm{d}y \ \Delta H_\epsilon(x,y), \quad A^- := \frac{1}{\lambda(\mathcal{J}^-)} \int_{\mathcal{J}^-} \mathrm{d}x\, \mathrm{d}y \ \Delta H_\epsilon(x,y). \tag{5.14}$$

On the complement of $\mathcal{J}^+ \cup \mathcal{J}^-$, ΔA_ϵ is equal to zero. We note that it is not necessary that $\lambda(\mathcal{J}^+) + \lambda(\mathcal{J}^-) = 1$. In what follows we show, using the strict convexity of I and Jensen's inequality, that, for a given ϵ and a perturbation term ΔH_ϵ,

$$I\left(T_1 + \Delta H_\epsilon\right) > I(T_1 + \Delta A_\epsilon). \tag{5.15}$$

Again, with a slight abuse of notation we use $I(\cdot)$ for the function defined on the graphon space and on the unit interval. Substituting the graphons and using the convexity of $I(\cdot)$ and Jensen's inequality yields

$$\begin{aligned} I(h_\epsilon^{*\downarrow}) = I(T_1 + \Delta H_\epsilon) &= \int_{[0,1]^2} \mathrm{d}x\, \mathrm{d}y \ I(T_1 + \Delta H_\epsilon(x,y)) \\ &= \int_{\mathcal{J}^+} \mathrm{d}x\, \mathrm{d}y \ I(T_1 + \Delta H_\epsilon(x,y)) + \int_{\mathcal{J}^-} \mathrm{d}x\, \mathrm{d}y \ I(T_1 + \Delta H_\epsilon(x,y)) \\ &> \lambda(\mathcal{J}^+) \ I\left(T_1 + \frac{1}{\lambda(\mathcal{J}^+)} \int_{\mathcal{J}^+} \mathrm{d}x\, \mathrm{d}y \ \Delta H_\epsilon(x,y)\right) \\ &\quad + \lambda(\mathcal{J}^-) \ I\left(T_1 + \frac{1}{\lambda(\mathcal{J}^-)} \int_{\mathcal{J}^-} \mathrm{d}x\, \mathrm{d}y \ \Delta H_\epsilon(x,y)\right) \\ &= \lambda(\mathcal{J}^+) \ I\left(T_1 + A^+\right) + \lambda(\mathcal{J}^-) \ I\left(T_1 + A^-\right) = I(T_1 + \Delta A_\epsilon), \end{aligned} \tag{5.16}$$

which proves (5.15). This argument shows that solving the variational problem $J^{\downarrow}(\epsilon)$ defined in (5.1) reduces to minimising $I(\cdot)$ amongst graphons taking two non-zero values and satisfying the two constraints (G_1) and (G_2) given in (5.10)–(5.11).

Step 2: In Step 1 we have shown that it suffices to restrict to graphons that can be written in the form $T_1 + g^*$, where g^* is a bounded, symmetric function defined on $[0,1]^2$, taking two non-zero values, i.e.,

$$g^* = g_+ 1_{\mathcal{J}^+} + g_- 1_{\mathcal{J}^-}, \tag{5.17}$$

for constants $g_+, g_- \in (-T_1, 1 - T_1)$ (depending on ϵ) and some sets $\mathcal{J}^+, \mathcal{J}^- \subset [0,1]^2$ (possibly depending on ϵ) with $0 < \lambda(\mathcal{J}^+), \lambda(\mathcal{J}^-) < 1$. For such a graphon we have

$$I(T_1 + g^*) = \lambda(\mathcal{J}^+) \ I(T_1 + g_+) + \lambda(\mathcal{J}^-) \ I(T_1 + g_-). \tag{5.18}$$

Note that the value of $I(T_1 + g^*)$ depends only on the size of the sets $\mathcal{J}^+, \mathcal{J}^-$. In what follows we analyse the variational problem of minimising $I(\cdot)$ among all piece-wise constant graphons, as defined above in (5.17), satisfying the constraints in (5.10) and (5.11). From (5.10) we obtain the first equation

$$g_+ \lambda(\mathcal{J}^+) = -g_- \lambda(\mathcal{J}^-). \tag{5.19}$$

Before moving to the constraint in (5.11) we show that it suffices to restrict ourselves to the class of graphons such that $\mathcal{J}^+ = I \times I$ and $\mathcal{J}^- = J \times J$ for some $I, J \subset [0,1]$. Consider the graphon g^* defined above in (5.17). For this given graphon we construct a graphon $\hat{g}^* = \hat{g}_+ 1_{I\times I} + \hat{g}_- 1_{J\times J}$ for some $\hat{g}_+ > 0, \hat{g}_- < 0, I, J \subset [0,1]$ such that

$$\hat{g}_+ \lambda(I)^2 = -\hat{g}_- \lambda(J)^2 \quad \text{and} \quad I(T_1 + g^*) > I(T_1 + \hat{g}^*). \tag{5.20}$$

Let $\hat{g}_+ = g_+$ and $\hat{g}_- = g_-$, and we choose I, J such that $\lambda(I)^2 < \lambda(\mathcal{J}^+)$, $\lambda(J)^2 < \lambda(\mathcal{J}^-)$ and $\frac{\lambda(I)^2}{\lambda(J)^2} = \frac{\lambda(\mathcal{J}^+)}{\lambda(\mathcal{J}^-)}$. Since $0 < \lambda(\mathcal{J}^+), \lambda(\mathcal{J}^-) < 1$ we can always chose such sets $I, J \subset [0,1]$. Using a Taylor expansion we get that

$$\begin{aligned} I(T_1 + g) - I(T_1 + \hat{g}) &= I'(T_1)(\lambda(\mathcal{J}^+) g_+ + \lambda(\mathcal{J}^-) g_- - \lambda(I)^2 \hat{g}_+ - \lambda(J)^2 \hat{g}_-) \\ &\quad + \tfrac{1}{2} I''(\xi_1)(\lambda(\mathcal{J}^+) - \lambda(I)^2) g_+^2 + \tfrac{1}{2} I''(\xi_2)(\lambda(\mathcal{J}^-) - \lambda(J)^2) g_-^2 \\ &= \tfrac{1}{2} I''(\xi_1)(\lambda(\mathcal{J}^+) - \lambda(I)^2) g_+^2 + \tfrac{1}{2} I''(\xi_2)(\lambda(\mathcal{J}^-) - \lambda(J)^2) g_-^2, \end{aligned} \tag{5.21}$$

for some $\xi_1 \in (T_1, T_1 + g_+)$ and $\xi_2 \in (T_1 + g_-, T_1)$. By convexity of $I(\cdot)$ we have that $I''(\xi_1) > 0$ and $I''(\xi_2) > 0$. Hence we have that

$$I(T_1 + g) > I(T_1 + \hat{g}), \tag{5.22}$$

which shows that we can restrict ourselves to graphons of the form

$$g^* = g_+ 1_{I\times I} + g_- 1_{J\times J}, \quad g_+ > 0,\ g_- < 0, \tag{5.23}$$

which satisfy the conditions in (5.10) and (5.11). We proceed with the condition in (5.11). A standard computation yields

$$\int_{[0,1]^3} \mathrm{d}x\, \mathrm{d}y\, \mathrm{d}z\ g^*(x,y) g^*(y,z) = \lambda(I)^3\, g_+^2 + \lambda(J)^3\, g_-^2 \tag{5.24}$$

and

$$\int_{[0,1]^3} \mathrm{d}x\, \mathrm{d}y\, \mathrm{d}z\ g^*(x,y) g^*(y,z) g^*(z,x) = \lambda(I)^3\, g_+^3 + \lambda(J)^3\, g_-^3. \tag{5.25}$$

Using the condition in (5.19), we get

$$\begin{aligned} &3T_1 \int_{[0,1]^3} \mathrm{d}x\, \mathrm{d}y\, \mathrm{d}z\ g^*(x,y) g^*(y,z) + \int_{[0,1]^3} \mathrm{d}x\, \mathrm{d}y\, \mathrm{d}z\ g^*(x,y) g^*(y,z) g^*(z,x) \\ &= g_-^2\, 3T_1 \frac{\lambda(J)^3}{\lambda(I)} (\lambda(J) + \lambda(I)) - g_-^3 \frac{\lambda(J)^3}{\lambda(I)^3} (\lambda(I)^3 - \lambda(J)^3) = 3T_1 \epsilon + o(\epsilon). \end{aligned} \tag{5.26}$$

There are multiple ways in which the condition in (5.26) can be met. We show that the lowest possible value of $I(\cdot)$ is attained when $g_+ \asymp \sqrt{\epsilon}, g_- \asymp -\sqrt{\epsilon}$ and $\lambda(I), \lambda(J)$ are constant. To that end we distinguish the following cases:

(I)

$$g_-^2\, 3T_1 \frac{\lambda(J)^3}{\lambda(I)} (\lambda(J) + \lambda(I)) \asymp \epsilon, \qquad g_-^3 \frac{\lambda(J)^3}{\lambda(I)^3} (\lambda(I)^3 - \lambda(J)^3) = o(\epsilon), \tag{5.27}$$

which splits into three subcases:

(Ia)

$$g_+ \asymp \epsilon^{1/2}, \quad g_- \asymp -\epsilon^{1/2}, \quad \frac{\lambda(J)}{\lambda(I)} \asymp 1. \tag{5.28}$$

(Ib)

$$g_+ \asymp \epsilon^{1/2+\delta/3}, \quad g_- \asymp -\epsilon^{1/2-\delta}, \quad \frac{\lambda(J)^3}{\lambda(I)} \asymp \epsilon^{2\delta}, \quad \delta \in (0, \tfrac{1}{2}]. \tag{5.29}$$

(Ic)

$$g_+ \asymp \epsilon^{1/2-3\delta}, \quad g_- \asymp -\epsilon^{1/2+\delta}, \quad \frac{\lambda(J)^3}{\lambda(I)} \asymp \epsilon^{-2\delta}, \quad \delta \in (0, \tfrac{1}{6}]. \tag{5.30}$$

(II)

$$g_-^2\, 3T_1 \frac{\lambda(J)^3}{\lambda(I)}(\lambda(J)+\lambda(I)) \asymp \epsilon^{1+\delta}, \quad -g_- \cdot \frac{1}{\lambda(I)^2} \asymp \epsilon^{-\delta}, \quad \delta > 0. \tag{5.31}$$

A simple calculation shows that in all four cases above $\lambda(I)+\lambda(J) \asymp 1$ and $\lambda(I)^3 - \lambda(J)^3 \asymp 1$ hence we can omit these two factors from the analysis below. In what follows we exclude cases (Ib), (Ic) and (II) one by one by comparing them to graphons of the type given in case (Ia).

Case Ib: We show that, for $\epsilon > 0$ sufficiently small, graphons having the structure indicated in (Ia) yield smaller values of the function $I(\cdot)$ than graphons with the structure in (Ib). We consider two graphons, denoted by $T_1 + g$ and $T_1 + \hat{g}$, where g is as in Case (Ia) and $\hat{g}$ is as in Case (Ib). Before giving the technical details of the proof, we present an intuitive argument why $I(T_1+g) < I(T_1+\hat{g})$. In what follows we will denote by $B(p)$ a Bernoulli random variable with parameter p. The function $-I(x)$, $x \in [0,1]$, defined in (2.27) represents the entropy of a $B(x)$ random variable with parameter x. On the graphon space the function $-I(h)$, $h \in W$, defined in (2.28) can be seen as the expectation of the entropy of a Bernoulli random variable with a random parameter (the expectation is with respect to the random parameter), i.e., $B(h(X,Y))$ with (X,Y) a uniformly distributed random variable on $[0,1]^2$. For $h \in W$ we have

$$-I(h) = \int_{[0,1]^2} \mathrm{d}x\, \mathrm{d}y\, [-I(h(x,y))] = \mathbb{E}[-I(h(X,Y))]. \tag{5.32}$$

Hence we have the following equivalence

$$I(T_1+g) < I(T_1+\hat{g}) \Leftrightarrow \mathbb{E}[-I(T_1+g(X,Y))] > \mathbb{E}[-I(T_1+\hat{g}(X,Y))], \tag{5.33}$$

where (X,Y) is a uniformly distributed random vector on $[0,1]^2$. Instead of working with entropy, it is intuitively simpler to work with the relative entropy with respect to the random variable $B(\frac{1}{2})$. The relative entropy is defined by

$$I_{\frac{1}{2}}(x) := x \log \frac{x}{\frac{1}{2}} + (1-x) \log \frac{1-x}{\frac{1}{2}}, \qquad x \in [0,1]. \tag{5.34}$$

Note that

$$\mathbb{E}[-I(T_1+g(X,Y))] > \mathbb{E}[-I(T_1+\hat{g}(X,Y))] \Leftrightarrow \mathbb{E}[I_{\frac{1}{2}}(T_1+g(X,Y))] < \mathbb{E}[I_{\frac{1}{2}}(T_1+\hat{g}(X,Y))]. \tag{5.35}$$

We first give an intuitive argument and afterwards prove that

$$\mathbb{E}[I_{\frac{1}{2}}(T_1+g(X,Y))] < \mathbb{E}[I_{\frac{1}{2}}(T_1+\hat{g}(X,Y))]. \tag{5.36}$$

We distinguish between two cases $T_1 \in (0, \frac{1}{2}]$ and $T_1 \in (\frac{1}{2}, 1]$. The case $T_1 \in (0, \frac{1}{2}]$ follows by using similar arguments as in case $T_1 \in (\frac{1}{2}, 1)$. We treat in detail only the case $T_1 \in (\frac{1}{2}, 1)$.

The relative entropy of a random variable with respect to $B(\frac{1}{2})$ is zero if and only if that random variable is equal to $B(\frac{1}{2})$. So, in order to compare the relative entropies in (5.36), we need to see how close the Bernoulli random variables with random parameters $T_1+g(X,Y)$ and $T_1+\hat{g}(X,Y)$ are to $B(\frac{1}{2})$. We are considering the case $T_1 > \frac{1}{2}$. Hence the random variables $B(T_1+g(X,Y))$ and $B(T_1+\hat{g}(X,Y))$ will be close to $B(\frac{1}{2})$ when the random parameters $T_1+g(X,Y)$ and $T_1+\hat{g}(X,Y)$ are close to $\frac{1}{2}$. This is the case when $g(X,Y)$ and $\hat{g}(X,Y)$ are negative. These events occur with probabilities

$$\mathbb{P}(T_1+g(X,Y) < T_1) = \mathbb{P}(g(X,Y) < 0) = \mathbb{P}(g(X,Y) = g_-) = \lambda(J)^2 \asymp 1, \tag{5.37}$$

because of the properties of the graphon in Case (Ia). Similarly, we have that

$$\mathbb{P}(T_1 + \hat{g}(X,Y) < T_1) = \mathbb{P}(\hat{g}(X,Y) < 0) = \mathbb{P}(\hat{g}(X,Y) = g_-) = \lambda(\hat{J})^2 \asymp \epsilon^{4\delta/3}, \tag{5.38}$$

for some $\delta \in (0, \frac{1}{2}]$, because of the properties of the graphon in Case (Ib). Hence we see that the random variable $B(T_1 + g(X,Y))$ is closer to the random variable $B(\frac{1}{2})$ with much higher probability than the random variable $B(T_1 + \hat{g}(X,Y))$. We can see this by computing the corresponding expectations,

$$\mathbb{E}(g(X,Y) \mid g(X,Y) = g_-)\, \mathbb{P}(g(X,Y) = g_-) = g_-\, \mathbb{P}(g(X,Y) = g_-) \asymp \epsilon^{1/2}, \tag{5.39}$$

while

$$\mathbb{E}(\hat{g}(X,Y) \mid \hat{g}(X,Y) = \hat{g}_-)\, \mathbb{P}(\hat{g}(X,Y) = \hat{g}_-) = \hat{g}_-\, \mathbb{P}(\hat{g}(X,Y) = \hat{g}_-) \asymp \epsilon^{1/2-\delta}\epsilon^{4\delta/3} = \epsilon^{1/2+\delta/3}. \tag{5.40}$$

In what follows we complete this argument by adding the technical details. We work out the expressions in the left-hand and right-hand sides of (5.36). The expression at the right-hand side of (5.36) can be written as

$$\mathbb{E}[I_{\frac{1}{2}}(T_1 + g(X,Y))] = L I_{\frac{1}{2}}(T_1 + g_+) + K I_{\frac{1}{2}}(T_1 + g_-) + (1 - L - K) I_{\frac{1}{2}}(T_1), \tag{5.41}$$

for some constants $L := \mathbb{P}(g(X,Y) = g_+)$ and $K = \mathbb{P}(g(X,Y) = g_-)$ independent of ϵ. Similarly,

$$\mathbb{E}[I_{\frac{1}{2}}(T_1 + \hat{g}(X,Y))] = \lambda(\hat{I})^2 I_{\frac{1}{2}}(T_1 + \hat{g}_+) + \epsilon^{4\delta/3} I_{\frac{1}{2}}(T_1 + \hat{g}_-) + (1 - \lambda(\hat{I})^2 - \epsilon^{4\delta/3}) I_{\frac{1}{2}}(T_1), \tag{5.42}$$

where $\lambda(\hat{I})^2 = \mathbb{P}(\hat{g}(X,Y) = \hat{g}_+) \asymp 1$ and $\mathbb{P}(\hat{g}(X,Y) = \hat{g}_-) \asymp \epsilon^{4\delta/3}$. Moreover, we recall that from the properties of the graphons in Case (Ia) and Case (Ib) we get

$$g_+ \asymp \sqrt{\epsilon}, \quad g_- \asymp -\sqrt{\epsilon}, \quad \hat{g}_+ \asymp \epsilon^{1/2+\delta/3}, \quad \hat{g}_- \asymp \epsilon^{1/2-\delta}, \quad \delta \in (0, \tfrac{1}{2}]. \tag{5.43}$$

Hence, for $T_1 \in (\frac{1}{2}, 1]$ and ϵ sufficiently small, because of (5.43), we obtain the following inequalities:

$$I_{\frac{1}{2}}(T_1 + g_+) > I_{\frac{1}{2}}(T_1 + \hat{g}_+) > I_{\frac{1}{2}}(T_1 + g_-) > I_{\frac{1}{2}}(T_1 + \hat{g}_-). \tag{5.44}$$

Using a Taylor expansion of the function $I(\cdot)$ around T_1 and the first order conditions

$$L g_+ + K g_- = 0 \quad \text{ and } \quad \lambda(\hat{I})^2 \hat{g}_+ + \lambda(\hat{J})^2 \hat{g}_- = 0, \tag{5.45}$$

we observe that (5.41) and (5.42) are equal to

$$\mathbb{E}[I_{\frac{1}{2}}(T_1 + g(X,Y))] = I_{\frac{1}{2}}(T_1) + \tfrac{1}{2} I''_{\frac{1}{2}}(T_1)(L g_+^2 + K g_-^2) + o\left(g_+^2 + g_-^2\right), \tag{5.46}$$

and

$$\mathbb{E}[I_{\frac{1}{2}}(T_1 + \hat{g}(X,Y))] = I_{\frac{1}{2}}(T_1) + \tfrac{1}{2} I''_{\frac{1}{2}}(T_1)(\lambda(\hat{I}^2)\hat{g}_+^2 + \lambda(\hat{J})^2 \hat{g}_-^2) + o\left(\lambda(\hat{I}^2)\hat{g}_+^2 + \lambda(\hat{J})^2 \hat{g}_-^2\right). \tag{5.47}$$

Using (5.43), we observe that $L g_+^2 + K g_-^2 \asymp \epsilon$ and $\lambda(\hat{I}^2)\hat{g}_+^2 + \lambda(\hat{J})^2 \hat{g}_-^2 \asymp \epsilon^{1+2\delta/3} + \epsilon^{4/3\delta}\epsilon^{1-2\delta} \asymp \epsilon^{1-2\delta/3}$. Hence for ϵ sufficiently small we observe that

$$\mathbb{E}\left[I_{\frac{1}{2}}(T_1 + g(X,Y))\right] < \mathbb{E}\left[I_{\frac{1}{2}}(T_1 + \hat{g}(X,Y))\right], \tag{5.48}$$

which proves (5.36).

Similar arguments can be used for the case $T_1 \in (0, \frac{1}{2})$ to show that graphons, as in Case (Ic), yield larger values of I for ϵ sufficiently small. We omit the details.

Case II: This case is simpler to exclude than the ones above. Indeed, suppose that (5.31) holds. Then either $\lambda(I)$ should become small or $-g_-$ should become large. But $g_- \asymp \epsilon^{-\delta}$ is not possible because g_- should stay bounded in $(-T_1, 0)$ as $\epsilon \downarrow 0$. Hence the only possibility is $\lambda(I) \asymp \epsilon^{\eta}$ and $g_- \asymp -\epsilon^{\zeta}$ for some η, ζ such that $\zeta - 2\eta = -\delta$, because of the second condition in (5.31). From the first condition in (5.31) we have that $2\zeta - \eta = 1 + \delta$. Solving these two equations we obtain that $\eta = \frac{1}{3} + \delta$ and $\zeta = \frac{2}{3} + \delta$. From (5.19) we get then that $g_+ \asymp \epsilon^{-\delta}$, which is not possible because g_+ should stay bounded in $(0, 1 - T_1)$ as $\epsilon \downarrow 0$.

At this point we summarise our findings. We have considered the variational problem $J^{\downarrow}(\epsilon)$ as given in (5.1) and we have shown that we can restrict ourselves to piecewise-constant graphons (see (5.17)) subject to the constraints in (5.10) and (5.11). Afterwards we have shown that we can restrict ourselves to an even smaller class of graphons, those of the form

$$g = g_+ 1_{I\times I} + g_- 1_{J\times J}, \tag{5.49}$$

for some $g_+ > 0$, $g_- < 0$ and $I, J \subset [0,1]$ with $\lambda(I)^2 + \lambda(J)^2 \leq 1$. More specifically, we have shown that the optimal perturbation will satisfy $g_+ \asymp \epsilon^{1/2}$, $g_- \asymp \epsilon^{1/2}$ and $\lambda(I) \asymp 1$, $\lambda(J) \asymp 1$. Then the solution to $J^{\downarrow}(\epsilon)$ has the form $T_1 + g^*\sqrt{\epsilon} + o(\epsilon)$, where $g^* = g_+ 1_{L\times L} + g_- 1_{K\times K}$, for some $g_+ > 0, g_- < 0, L, K \in (0,1)$ independent of ϵ, is a symmetric function defined on $[0,1]^2$. From the constraints (5.10) and (5.11) we have that $g_+ L^2 = -g_- K^2$ and $L^3 g_+^2 + K^3 g_-^2 = 1$. A simple calculation shows that

$$\begin{aligned} I(T_1 + g\sqrt{\epsilon}\,) &= I(T_1) + I'(T_1)(L^2 g_+ + K^2 g_-)\sqrt{\epsilon} + \tfrac{1}{2} I''(T_1)(L^2 g_+^2 + K^2 g_-^2)\epsilon + o(\epsilon) \\ &= I(T_1) + \tfrac{1}{2} I''(T_1)(L^2 g_+^2 + K^2 g_-^2)\epsilon + o(\epsilon). \end{aligned}$$

Hence, in order to find the optimal graphon we need to solve the following optimisation problem:

$$\begin{aligned} &\min \left(L^2 g_+^2 + K^2 g_-^2\right) \\ &\text{such that } L + K \leq 1, \quad g_+ L^2 + g_- K^2 = 0, \quad L^3 g_+^2 + K^3 g_-^2 = 1. \end{aligned} \tag{5.50}$$

This is equivalent to

$$\begin{aligned} &\min \left(\frac{1}{K} + \frac{1}{L} - \frac{2}{K+L}\right) \\ &\text{such that } L + K \leq 1. \end{aligned} \tag{5.51}$$

From a standard computation we find that the optimal K, L should satisfy $K + L = 1$. Hence we need to minimize $\frac{1-2L+L^2}{L(1-L)}$. This function is convex in $L \in (0,1)$ and attains a unique minimum at the point $L = \frac{1}{2}$. Having computed L, K we find $g_+ = -g_- = 2$, and the optimal solution to $J^{\downarrow}(\epsilon)$, for ϵ sufficiently small, is the graphon

$$h_\epsilon^{*\downarrow}(x,y) = \begin{cases} T_1 + 2\sqrt{\epsilon}, & \text{if } (x,y) \in [0, \frac{1}{2}]^2, \\ T_1, & \text{if } (x,y) \in [0, \frac{1}{2}] \times (\frac{1}{2}, 1] \text{ or } (\frac{1}{2}, 1] \times [0, \frac{1}{2}], \\ T_1 - 2\sqrt{\epsilon}, & \text{if } (x,y) \in (\frac{1}{2}, 1]^2. \end{cases} \tag{5.52}$$

A standard computation shows that $T_1(h_\epsilon^{*\downarrow}) = T_1$ and $T_2(h_\epsilon^{*\downarrow}) = T_1^3 + 3T_1\epsilon$.

5.2 Proof of Lemmas 5.2–5.3

In this section we provide the technical details leading to the optimal perturbation of the variational problem in (5.2). We denote one of the, possibly multiple, optimizers of (5.2) by $\tilde{h}_\epsilon^{*\uparrow}$. In the proof, in order to keep the notation light, we will consider a representative element of this class, denoted by $h_\epsilon^{*\uparrow}$. We start by writing the optimizer in the form $h_\epsilon^{*\uparrow} = T_1 + \Delta H_\epsilon$ for some perturbation term ΔH_ϵ. The perturbation term has to be a bounded symmetric function defined on the unit square $[0,1]^2$ taking values in $\mathbb{R}$. The optimizer $h_\epsilon^{*\uparrow}$ has to satisfy the constraints

$$T_1(h_\epsilon^{*\uparrow}) = T_1 \qquad \text{and} \qquad T_2(h_\epsilon^{*\uparrow}) = T_1^3 - T_1^3\epsilon, \tag{5.53}$$

and so the perturbation ΔH_ϵ needs to satisfy the two constraints

$$(K_1): \int_{[0,1]^2} \mathrm{d}x\,\mathrm{d}y\ \Delta H_\epsilon(x,y) = 0, \tag{5.54}$$

and

$$\begin{aligned}(K_2): \ 3T_1 &\int_{[0,1]^3} \mathrm{d}x\,\mathrm{d}y\,\mathrm{d}z\ \ \Delta H_\epsilon(x,y)\Delta H_\epsilon(y,z) \\ &+ \int_{[0,1]^3} \mathrm{d}x\,\mathrm{d}y\,\mathrm{d}z\ \ \Delta H_\epsilon(x,y)\Delta H_\epsilon(y,z)\Delta H_\epsilon(z,x) = -T_1^3\epsilon.\end{aligned} \tag{5.55}$$

We observe that the construction above in Section 5.1 is no longer possible in the present case, because the first integral in (5.55) is always nonnegative (think of it as a quadratic form), i.e., for every symmetric function $\Delta H_\epsilon\colon [0,1]^2 \to \mathbb{R}$

$$\int_{[0,1]^3} \mathrm{d}x\,\mathrm{d}y\,\mathrm{d}z\,\Delta H_\epsilon(x,y)\Delta H_\epsilon(y,z) \geq 0. \tag{5.56}$$

Hence, in order to get the condition in (5.55), both integrals must contribute and both must be asymptotically on the order of ϵ. In other words, there is competition between the two integrals in (5.55), which we did not have in the previous perturbation. We show that the cheapest way to achieve such a constraint is by considering a *local perturbation*, as indicated in (4.24) and in Lemma 5.2. A global perturbation as in (3.5) or a combination of a local and a global perturbation will not work, because the first integral will be of higher order than the second integral in (5.55). Hence the optimal way to achieve the constraints in (5.54) and in (5.55) is by considering a local perturbation of the form

$$h_\epsilon^{*\uparrow} = T_1\, 1_{[0,1]^2\setminus\square_\epsilon} + g^*_{\square_\epsilon}, \tag{5.57}$$

where the region $\square_\epsilon = [0,\epsilon^{1/3}]^2$ and the function g^* is given by

$$g^*_{\square_\epsilon}(x,y) := \begin{cases} 2T_1, & 0 < x < \frac{1}{2}\epsilon^{1/3} < y < \epsilon^{1/3} \text{ or } 0 < y < \frac{1}{2}\epsilon^{1/3} < x < \epsilon^{1/3}, \\ 0 & \text{otherwise.}\end{cases} \tag{5.58}$$

Proof of Lemma 5.2: In what follows we provide the technical details leading to (5.57), thereby proving the result in Lemma 5.2. As before, we write the optimal graphon $h_\epsilon^{*\uparrow}$ in the form $T_1 + \Delta H_\epsilon$ for some symmetric function ΔH_ϵ defined on $[0,1]^2$. We show that the optimal graphon $h_\epsilon^{*\uparrow}$ is constant everywhere on $[0,1]^2$. This means that, for every function $f(\epsilon)$ of ϵ such that $f(\epsilon) \downarrow 0$ when $\epsilon \downarrow 0$, we must have $(\Delta H_\epsilon(x,y)\cdot f(\epsilon)) \downarrow 0$ for every $(x,y) \in [0,1]^2$ as $\epsilon \downarrow 0$. Suppose that there exists some set $\mathcal{I} \subset [0,1]^2$ such that $\Delta H_\epsilon \asymp f(\epsilon)$, for some function $f(\cdot)$. Then

$$\int_{\mathcal{I}} \mathrm{d}x\ \mathrm{d}y\ \Delta H_\epsilon(x,y) = f(\epsilon)\lambda(\mathcal{I}). \tag{5.59}$$

From the integral condition in (5.54) we see that there must exist a set $\bar{\mathcal{I}} \subset [0,1]^2$ such that

$$\int_{\bar{\mathcal{I}}} \mathrm{d}x\ \mathrm{d}y\ \Delta H_\epsilon(x,y) = -f(\epsilon)\lambda(\mathcal{I}). \tag{5.60}$$

Then the optimiser $h_\epsilon^{*\uparrow}$ can be written, for $(x,y) \in [0,1]^2$, as

$$h_\epsilon^{*\uparrow}(x,y) = T_1 + f(\epsilon)1_{\mathcal{I}}(x,y) + \Delta H_\epsilon(x,y)1_{\bar{\mathcal{I}}}(x,y) + \Delta H_\epsilon(x,y)1_{[0,1]^2\setminus\mathcal{I}\cup\bar{\mathcal{I}}}(x,y). \tag{5.61}$$

Next consider the following graphon

$$\bar{h}_\epsilon^* = T_1 1_{\mathcal{I}\cup\bar{\mathcal{I}}} + (T_1 + \Delta H_\epsilon)1_{[0,1]^2\setminus\mathcal{I}\cup\bar{\mathcal{I}}}. \tag{5.62}$$

In what follows, with a slight abuse of notation, we write $I(\cdot)$ to denote the function defined on the graphon space and on the unit interval (see (2.27) and (2.28)). We have

$$\begin{aligned}
I(h_\epsilon^{*\uparrow}) &= \int_{[0,1]^2} \mathrm{d}x\,\mathrm{d}y\; I(h_\epsilon^{*\uparrow}(x,y)) \\
&= I(T_1 + f(\epsilon))\,\lambda(\mathcal{I}) + \int_{\bar{\mathcal{I}}} \mathrm{d}x\,\mathrm{d}y\; I(T_1 + \Delta H_\epsilon(x,y)) + \int_{[0,1]^2\setminus\mathcal{I}\cup\bar{\mathcal{I}}} \mathrm{d}x\,\mathrm{d}y\; I(T_1 + \Delta H_\epsilon(x,y)) \\
&> I(T_1 + f(\epsilon))\,\lambda(\mathcal{I}) + I\left(T_1 + \frac{1}{\lambda(\bar{\mathcal{I}})}\int_{\bar{\mathcal{I}}} \mathrm{d}x\,\mathrm{d}y\; \Delta H_\epsilon(x,y)\right)\lambda(\bar{\mathcal{I}}) \\
&\quad + \int_{[0,1]^2\setminus\mathcal{I}\cup\bar{\mathcal{I}}} \mathrm{d}x\,\mathrm{d}y\; I(T_1 + \Delta H_\epsilon(x,y)) \\
&= I(T_1 + f(\epsilon))\,\lambda(\mathcal{I}) + I\left(T_1 - \frac{1}{\lambda(\bar{\mathcal{I}})} f(\epsilon)\lambda(\mathcal{I})\right)\lambda(\bar{\mathcal{I}}) + \int_{[0,1]^2\setminus\mathcal{I}\cup\bar{\mathcal{I}}} \mathrm{d}x\,\mathrm{d}y\; I(T_1 + \Delta H_\epsilon(x,y)) \\
&> \big(\lambda(\mathcal{I}) + \lambda(\bar{\mathcal{I}})\big)\, I\left(T_1 + f(\epsilon)\frac{\lambda(\mathcal{I})}{\lambda(\mathcal{I}) + \lambda(\bar{\mathcal{I}})} - f(\epsilon)\frac{\lambda(\mathcal{I})}{\lambda(\mathcal{I}) + \lambda(\bar{\mathcal{I}})}\right) \\
&\quad + \int_{[0,1]^2\setminus\mathcal{I}\cup\bar{\mathcal{I}}} \mathrm{d}x\,\mathrm{d}y\; I(T_1 + \Delta H_\epsilon(x,y)) \\
&= \big(\lambda(\mathcal{I}) + \lambda(\bar{\mathcal{I}})\big)\, I(T_1) + \int_{[0,1]^2\setminus\mathcal{I}\cup\bar{\mathcal{I}}} \mathrm{d}x\,\mathrm{d}y\; I(T_1 + \Delta H_\epsilon(x,y)) \\
&= I(\bar{h}_\epsilon^*),
\end{aligned} \tag{5.63}$$

where the first inequality follows from Jensen's inequality and the strict convexity of $I(\cdot)$, the second equality holds because of (5.60). Thus, we see that the optimal graphon must be equal to T_1 on a as large as possible domain, so that the constraints in (5.54) and (5.55) are satisfied. Hence the optimal graphon will have the form

$$h_\epsilon^{*\uparrow} = T_1 1_{[0,1]^2\setminus I_\epsilon\times I_\epsilon} + g_\epsilon 1_{I_\epsilon\times I_\epsilon}, \tag{5.64}$$

for some $I_\epsilon \subset [0,1]$ and some non-negative symmetric function g on $I_\epsilon \times I_\epsilon$. A similar reasoning as in (5.22) can be applied to show that we may restrict ourselves to sets have a product form. In order to keep the notation light we omit the dependence of g and the interval I on ϵ. The function g has to be symmetric and non-negative because the graphon $h_\epsilon^{*\uparrow}$ has to be symmetric and take values in $[0,1]$. Furthermore, the sets I and the function g have to be such so that the graphon $h_\epsilon^{*\uparrow}$ satisfies the constraints, i.e., $T_1(h_\epsilon^{*\uparrow}) = T_1$ and $T_2(h_\epsilon^{*\uparrow}) = T_1^3 - T_1^3\epsilon$. A standard computation shows that g must satisfy the integral conditions

$$\int_{I\times I} \mathrm{d}x\,\mathrm{d}y\; g(x,y) = T_1\lambda(I)^2, \qquad \int_{I\times I\times I} \mathrm{d}x\,\mathrm{d}y\,\mathrm{d}z\; g(x,y)g(y,z)g(z,x) = (\lambda(I)^3 - \epsilon)T_1^3. \tag{5.65}$$

Consider the graphon $g^*_{\square_\epsilon}$ defined in (5.58), i.e., for $(x,y) \in [0,1]^2$,

$$g^*_{\square_\epsilon}(x,y) := \begin{cases} 2T_1, & 0 < x < \frac{1}{2}\epsilon^{1/3} < y < \epsilon^{1/3} \text{ or } 0 < y < \frac{1}{2}\epsilon^{1/3} < x < \epsilon^{1/3}, \\ 0, & \text{otherwise}, \end{cases} \tag{5.66}$$

where $\square_\epsilon = [0,\epsilon^{1/3}]^2$. Standard computations show that $\lambda(I) = \epsilon^{1/3}$, $\lambda(\square_\epsilon) = \epsilon^{2/3}$ and that $g^*_{\square_\epsilon}$ satisfies the integral conditions in (5.65). The final step is to show that we cannot find a graphon that performs better than $g^*_{\square_\epsilon}$. As mentioned above (5.64), we want to maximise the area of the domain where $h_\epsilon^{*\uparrow}$ is equal to T_1. Hence we have to exclude the following two cases:

(1) There exists a set $J \subset [0,1]$ with $\lambda(J) < \epsilon^{1/3}$ and a non-negative symmetric function g defined on $J \times J$ that performs better than $g^*_{\square_\epsilon}$.

(2) There exists a set $J \subset [0,1]$ with $\lambda(J) = \epsilon^{1/3}$ and a non-negative symmetric function g defined on $J \times J$ that performs better than $g^*_{\square_\epsilon}$.

We start with (1). Suppose that there exist such J and g. Then from the second condition in (5.65) we have that

$$\int_{J\times J\times J} \mathrm{d}x\,\mathrm{d}y\,\mathrm{d}z\ g(x,y)g(y,z)g(z,x) = (\lambda(J)^3 - \epsilon)\,T_1^3 < 0, \tag{5.67}$$

since $\lambda(J) < \epsilon^{1/3}$. This can happen only if g can take negative values. This contradicts the fact that g must be non-negative. We proceed with (2). Again, from the second condition in (5.65) we get that g must satisfy the integral condition

$$\int_{J\times J\times J} \mathrm{d}x\,\mathrm{d}y\,\mathrm{d}z\ g(x,y)g(y,z)g(z,x) = (\lambda(I)^3 - \epsilon)\,T_1^3 = 0. \tag{5.68}$$

Hence the function g has a bipartite structure on $J \times J$, which again leads to the graphon g^*_ϵ.

Proof of Lemma 5.3: For the proof of Lemma 5.3 the reasoning is similar. The difference lies in the last step, where instead of the graphon in (5.58) we need to consider the graphon defined in (3.10), for $\ell \in \mathbb{N}\backslash\{1\}$ and $T_1 \in (\frac{\ell-1}{\ell}, \frac{\ell}{\ell+1}]$. Up to (5.65) the proof carries on without any difference. Using a similar argument as before we can exclude the case $\lambda(I) < \epsilon^{1/3}$ showing that $\square_\epsilon := I \times I = [0, \epsilon^{1/3}]^2$. A standard computation shows that

$$I(h^{*\uparrow}_\epsilon) = I(T_1)(1-\epsilon^{2/3}) + I(g^*_{\square_\epsilon})\epsilon^{2/3}. \tag{5.69}$$

In order to find the optimal $g^*_{\square_\epsilon}$, we need to minimize $I(g)$ among all graphons defined on $[0,\epsilon^{1/3}]^2$ satisfying

$$\int_{[0,\epsilon^{1/3}]^2} \mathrm{d}x\,\mathrm{d}y\ g(x,y) = T_1\epsilon^{2/3}, \qquad \int_{[0,\epsilon^{1/3}]^3} \mathrm{d}x\,\mathrm{d}y\,\mathrm{d}z\ g(x,y)g(y,z)g(z,x) = 0. \tag{5.70}$$

Consider, for $\ell \in \mathbb{N}\backslash\{1\}$, the graphon in (2.33). We know that this graphon minimizes I among all graphons defined on $[0,1]^2$ satisfying

$$\int_{[0,1]^2} \mathrm{d}x\mathrm{d}y\ g(x,y) = T_1, \qquad \int_{[0,1]^3} \mathrm{d}x\,\mathrm{d}y\,\mathrm{d}z\ g(x,y)g(y,z)g(z,x) = 0. \tag{5.71}$$

Hence we see that the optimal graphon $g^*_{\square_\epsilon}$ will have the same structure as the graphon in (2.33) but 'squeezed' in the interval $[0,\epsilon^{1/3}]^2$. This is exactly the graphon defined in (3.10).

References

[1] D. Aristoff and L. Zhu, Asymptotic structure and singularities in constrained directed graphs, Stoch. Proc. Appl. 125 (2011) 4154–4177.

[2] D. Aristoff and L. Zhu, On the phase transition curve in a directed exponential random graph model, Adv. Appl. Prob. 50 (2018) 272–301.

[3] S. Bhamidi, G. Bresler and A. Sly, Mixing time of exponential random graphs, Ann. Appl. Probab. 21 (2011) 2146–2170.

[4] C. Borgs, J.T. Chayes, L. Lovász, V.T. Sós and K. Vesztergombi, Convergent graph sequences I: Subgraph frequencies, metric properties, and testing, Adv. Math. 219 (2008) 1801–1851.

[5] C. Borgs, J.T. Chayes, L. Lovász, V.T. Sós and K. Vesztergombi, Convergent sequences of dense graphs II: Multiway cuts and statistical physics, Ann. Math. 176 (2012) 151–219.

[6] S. Chatterjee and A. Dembo, Non linear large deviations, Adv. Math. 299 (2016) 396–450.

[7] S. Chatterjee and P. Diaconis, Estimating and understanding exponential random graph models, Ann. Stat. 41 (2013) 2428–2461.

[8] S. Chatterjee, P. Diaconis and A. Sly, Random graphs with a given degree sequence, Ann. Appl. Probab. 21 (2011) 1400–1435.

[9] S. Chatterjee and S.R.S. Varadhan, The large deviation principle for the Erdős-Rényi random graph, European J. Comb. 32 (2011) 1000–1017.

[10] A. Dembo and E. Lubetzky, A large deviations principle for the Erdős-Rényi uniform random graph, arXiv: 1804.11327 (2018)

[11] P. Diao, D. Guillot, A. Khare and B. Rajaratnam, Differential calculus on graphon space, J. Combin. Theory Ser. A 133 (2015) 183–227.

[12] J.W. Gibbs, *Elementary Principles of Statistical Mechanics*, Yale University Press, New Haven, Connecticut, 1902.

[13] G. Garlaschelli, F. den Hollander and A. Roccaverde, Ensemble equivalence in random graphs with modular structure, J. Phys. A: Math. Theor. 50 (2017).

[14] G. Garlaschelli, F. den Hollander and A. Roccaverde, Covariance structure behind breaking of ensemble equivalence, to appear in J. Stat. Phys.,

[15] F. den Hollander, M. Mandjes, A. Roccaverde and N.J. Starreveld, Ensemble equivalence for dense graphs, Electronic J. Prob. 23 (2018), Paper no. 12, 1–26.

[16] E.T. Jaynes, Information theory and statistical mechanics, Phys. Rev. 106 (1957) 620–630.

[17] R. Kenyon, C. Radin, K. Ren and L. Sadun, Multipodal structure and phase transitions in large constrained graphs, J. Stat. Phys. 168 (2017) 233–258.

[18] R. Kenyon, C. Radin, K. Ren and L. Sadun, The phases of large networks with edge and triangle constraints, J. Phys. A: Math. Theor. 50 (2017).

[19] R. Kenyon and M. Yin, On the asymptotics of constrained exponential random graphs, J. Appl. Prob. 54 (2017) 165–180.

[20] E. Lubetzky and Y. Zhao, On replica symmetry of large deviations in random graphs, Random Struct. and Algor. 47 (2015) 109–146.

[21] E. Lubetzky and Y. Zhao, On the variational problem for upper tails in sparse random graphs, Random Struct. and Algor. 50 (2017) 420–436.

[22] R. Mavi and M. Yin, Ground states for exponential random graphs, J. Math. Phys., 59 (2018) 013303.

[23] J. Park and M.E.J. Newman, Solution to the 2-star model of a network, Phys. Rev. E 70 (2004) 066146.

[24] O. Pikhurko and A. Razborov, Asymptotic structure of graphs with the minimum number of triangles, Comb. Prob. Comp. 26 (2017) 138–160.

[25] C. Radin, K. Ren and L. Sadun, Surface effects in dense random graphs with sharp edge constraints, arXiv: 1709.01036, (2018).

[26] C. Radin and L. Sadun, Phase transitions in a complex network, J. Phys. A: Math. Theor. 46 (2013) 305002.

[27] C. Radin and L. Sadun, Singularities in the entropy of asymptotically large simple graphs, J. Stat. Phys. 158 (2015) 853–865.

[28] C. Radin and M. Yin, Phase transitions in exponential random graphs, Ann. Appl. Probab. 23 (2013) 2458–2471.

[29] A.A. Razborov, On the minimal density of triangles in graphs, Comb. Probab. Comput. (2008) 10.1017.

[30] T. Squartini and D. Garlaschelli, Reconnecting statistical physics and combinatorics beyond ensemble equivalence, [arXiv:1710.11422].

[31] T. Squartini, J. de Mol, F. den Hollander and D. Garlaschelli, Breaking of ensemble equivalence in networks, Phys. Rev. Lett. 115 (2015) 268701.

[32] H. Touchette, Equivalence and nonequivalence of ensembles: Thermodynamic, macrostate, and measure levels, J. Stat. Phys. 159 (2015) 987–1016.

[33] M. Yin, Critical phenomena in exponential random graphs, J. Stat. Phys. 153 (2013) 1008–1021.

[34] M. Yin, Large deviations and exact asymptotics for constrained exponential random graphs, Electron. Commun. Probab. 20 (2015) 1–14.

[35] M. Yin and L. Zhu, Asymptotics for sparse exponential random graph models, Braz. J. Probab. Stat. 31 (2017) 394–412.

[36] L. Zhu, Asymptotic Structure of constrained exponential random graph models, J. Stat. Phys. 166 (2017) 1464–1482.